Geofísica Internacional (2025) **64-3**: 1691 - 1717

Pre-eruptive conditions of a magma mixing-assimilation systems at La Malinche volcano, Mexico

Johana Andrea Gómez-Arango[1,2]*, Giovanni Sosa-Ceballos[2], Mario E. Boijseauneau-López[3]

Abstract

The pre-eruptive conditions of Holocene-Pleistocene magma reservoir of La Malinche volcano, México, remain misunderstood. La Malinche eruptions including Huamantla (>45000 yrs.), Malinche I (21500 yrs.), and Malinche II (12000-9000 yrs.) are relevant to evaluate the hazard due to their explosive behavior and its closeness with Puebla, Huamantla and Tlaxcala cities (2 million people in a radius of 30 kilometers). Huamantla, Malinche I and Malinche II deposits consist of pumice falls recording Plinian eruptions. Here we present the result of a study on the pre-eruptive conditions (pressure, temperature) of Late Pleistocene-Holocene La Malinche reservoirs through geothermobarometers (amphibole, Fe-Ti oxides and melt inclusions hosted in phenocrystals of plagioclase). We compare mineral stability diagrams, geothermobarometry and mineral chemistry data and results with literature cases. Pumice fragments in all deposits show a mineral assembly of plagioclase, biotite, amphibole and Fe - Ti oxides megacrystals (>1 cm), phenocrystals (1000-300 μm) and microcrystals (<300 μm). At least one population show disequilibrium features such as sieve, zoning and resorption edges. We suggest that La Malinche magmas evolved through magma mixing and assimilation processes. Here we present an exhaustive analysis aimed to identify the most likely equilibrium phases and obtain information about the storage pressure and temperature throughout geothermobarometry. We performed a bibliographic analysis of phase diagrams that match La Malinche magmas composition before mixing-assimilation occurred. We conclude that the Late Pleistocene-Holocene La Malinche melts were stored at ~7.7-10.3 km depth (~200±70 MPa) and at a temperature of ~820±10 °C. Similar reservoir depths have been previously proposed for the Sierra Nevada volcanic range in central Mexico, which is close to La Malinche volcano.

Key words: La Malinche volcano; Pre-eruptive conditions, Plinian activity; Assimilation; Magma Mixing.

Resumen

Las condiciones pre-eruptivas del reservorio magmático del Holoceno-Pleistoceno del volcán La Malinche, México, siguen siendo poco comprendidas. Las erupciones de La Malinche, incluyendo Huamantla (>45,000 años), Malinche I (21,500 años) y Malinche II (12,000-9,000 años), son relevantes para evaluar el riesgo debido a su comportamiento explosivo y su proximidad a las ciudades de Puebla, Huamantla y Tlaxcala (2 millones de personas en un radio de 30 kilómetros). Los depósitos de Huamantla, Malinche I y Malinche II consisten en caídas de pómez que registran erupciones plinianas. En este trabajo presentamos los resultados de un estudio sobre las condiciones pre-eruptivas (presión, temperatura) de los reservorios del Pleistoceno Tardío-Holoceno de La Malinche mediante geotermobarómetros (anfíbol, óxidos de Fe-Ti) e inclusiones de fundido atrapadas en fenocristales de plagioclasa. Comparamos diagramas de fase, datos geotermométricos y de química mineral con casos reportados en la literatura. Los fragmentos de pómez en todos los depósitos presentan una asociación mineral de plagioclasa, biotita, anfíbol y óxidos de Fe-Ti, con megacristales (>1 cm), fenocristales (1000-300 μm) y microcristales (<300 μm). Al menos una población muestra características de desequilibrio, como texturas tamiz, zonación y bordes de resorción. Proponemos que los magmas de La Malinche evolucionaron mediante procesos de mezcla de magmas y asimilación. Aquí presentamos un análisis exhaustivo dirigido a identificar las fases más probables en equilibrio y obtener información sobre las condiciones de presión y temperatura a través de geotermobarometría. Realizamos un análisis bibliográfico de diagramas de estabilidad mineral que coinciden con la composición de los magmas de La Malinche antes de que ocurriera la mezcla-asimilación. Concluimos que los fundidos del Pleistoceno Tardío-Holoceno de La Malinche estuvieron almacenados a una profundidad de ~7.7-10.3 km (~200±70 MPa) y a una temperatura de ~820±10 °C. Profundidades similares de reservorios han sido propuestas previamente para la Sierra Nevada, un complejo volcánico cercano al volcán La Malinche en el centro de México.

Palabras clave: Volcán La Malinche; Condiciones pre-eruptivas; Actividad pliniana; Asimilación; Mezcla de magmas.

Received: December 7, 2024; Accepted: June 5, 2025; Published on-line: July 1, 2025.

Editorial responsibility: Dr. Roberto Carniel

* Corresponding author: Johana Andrea Gómez-Arango, johanagomezarango@comunidad.unam.mx
[1] Universidad Nacional Autónoma de México, Escuela Nacional de Estudios Superiores Campus Morelia, Posgrado en Ciencias de la Tierra, Morelia-Michoacán, México
[2] Universidad Nacional Autónoma de México, Instituto de Geofísica, Unidad Michoacán, Morelia-Michoacán, México.
[3] Universidad Nacional Autónoma de México, Escuela Nacional de Estudios Superiores, Campus Morelia, Morelia-Michoacán, México.

https://doi.org/10.22201/igeof.2954436xe.2025.64.3.1849

1. Introduction

Highly explosive eruptions, such as Plinian and Ultra-Plinian eruptions, pose a serious volcanic hazard and are a major cause of human casualties(e.g., Chichon volcano in Sigurdsson, 1984; Vesuvius and Santorini in Barberi and Carapezza, 2019). Thus, studies on the pre-eruptive conditions (temperature, pressure and volatile content) of magma involved in explosive eruptions are critical and allow us to obtain relevant information on the plumbing system of active volcanoes. Pre-eruptive conditions control the rheology of magmas and, consequently, may affect the eruptive dynamics (explosive vs effusive), and the crystallization of mineral phases (e.g., Spilliaert *et al.*, 2006; Ginibre *et al.*, 2007; Cassidy *et al.*, 2018; Arzilli *et al.*, 2019; Cooper, 2019; Arzilli *et al.*, 2022; La Spina *et al.*, 2022; Bonechi *et al.*, 2024). Volcanic eruptions cannot be prevented, but a better understanding on how explosive volcanoes work can be reached through petrological, geophysical and geochemical studies.

Common petrological tools include mineral geothermobarometry, melt inclusions, numerical methods and laboratory experiments (e.g., Gardner *et al.*, 1995; Gurenko *et al.*, 2005; Spilliaert *et al.*, 2006; Goepfert and Gardner, 2010; Lohmar *et al.*, 2012; Muir *et al.*, 2014; Pelullo *et al.*, 2022).

However, all of these methodologies have limitations and statements that must be considered, especially for non-equilibrium mineral phases related to evolution processes as magma mixing and assimilation of country/hydrothermal rocks. Although natural magmas often depart from equilibrium conditions, and laboratory experiments have inherent limitations when extrapolating to magma reservoir scales, pre-eruptive conditions can provide valuable snapshots of pressure-temperature regimes for resident magmas (Eskandari *et al.*, 2018; Pelullo *et al.*, 2022). Therefore , the results have the significance of a best possible approximation. The estimate of the pre-eruptive conditions of intermediate magmas is an issue commonly discussed in the scientific literature (e.g., Blatter and Carmichael, 1998; Moore and Carmichael, 1998; Blatter and Carmichael, 2001). However, there is a lack of consensus on the impact of the thermodynamic and chemical disequilibrium on these estimates, suggesting that pre-eruptive conditions may vary significantly within the plumbing systems of volcanoes. Furthermore, if intermediate rocks contain amphibole and/or biotite (as they commonly do), it becomes impossible to accurately model these magmas using computational tools such as MELTS (Gualda and Ghiorso, 2015). This is because MELTS relies on thermodynamic models that currently do not adequately account for the solid-solution behavior of amphiboles (particularly calcic varieties) or the water-dependent stability of biotite, leading to significant uncertainties in phase equilibria calculations (Gualda and Ghiorso, 2015).

La Malinche volcano erupted andesitic to dacitic magmas. It is a stratovolcano located in the central-eastern sector of the Trans-Mexican Volcanic Belt, about 25 km northeast of the city of Puebla, in the states of Puebla and Tlaxcala (Figure 1A). La Malinche is one of the highest volcanoes in Mexico (4,461 meters above sea level (Figure 1B) and represents a potentially hazardous volcano (Macías, 2007; Castro-Govea and Siebe, 2007) because the number of inhabitants (at least two million people) located in its surroundings. La Malinche volcano has experienced at least three explosive eruptions (Plinian pumice fallout) since the end of Pleistocene (Castro-Govea and Siebe, 2007). La Malinche, as all other andesitic-dacitic volcanic systems, shows mineralogical and geochemical evidences of disequilibrium (Castro-Govea, 2007; Espinosa *et al.*, 2021). Therefore, the determination of the pre-eruptive conditions of La Malinche Holocene reservoir yields two possibilities: a) estimate P-T conditions without a rigorous analysis of the magmatic processes; b) recognize that mixing and assimilation control the final composition of the rock implying non-equilibrium conditions. The estimate of the pre-eruptive conditions of non-equilibrium magmas could be calibrated using multiples methodologies (i.e., Arce *et al.*, 2013), which could provide a realistic approach to the estimate of the T, P, and depth of magma storage before eruption.

Here we define the depth of La Malinche magmatic reservoir of the recognized Plinian eruptions (Huamantla, Malinche I and Malinche II Pumice) and the associated evolution processes based on mineral-glass chemistry, geothermobarometry (amphibole, Fe-Ti oxides) and virtual mineral stability diagrams based on the experimental data on arc volcanoes. We discuss the applicability of these approaches in the case of to non-equilibrium systems. We made a comparison of La Malinche's pre-eruptive conditions with those of Popocatépetl volcano and other volcanoes of the Sierra Nevada Volcanic Range (located 65 km to the west) to investigate if there is a pattern in the storage conditions of magma reservoirs within this zone of the Trans-Mexican Volcanic Belt.

2. Background

Few studies have been focused on La Malinche volcano, with most investigations addressing its eruptive history (Castro-Govea, 1999; Castro-Govea and Siebe, 2007), the associated hazards (Heine, 1971; Heine and Heide-Weise, 1973; Werner, 1976; Castro-Govea and Siebe, 2007), glacier and paleoenvironmental studies (Heine, 1984, 1988), and geomorphological studies (Castillo-Rodríguez *et al.*, 2010).. However, the magnitude of its explosive eruptions remains largely unexplored, and only recently have studies begun to investigate the pre-eruptive conditions of a specific eruption (Espinosa *et al.*, 2021).

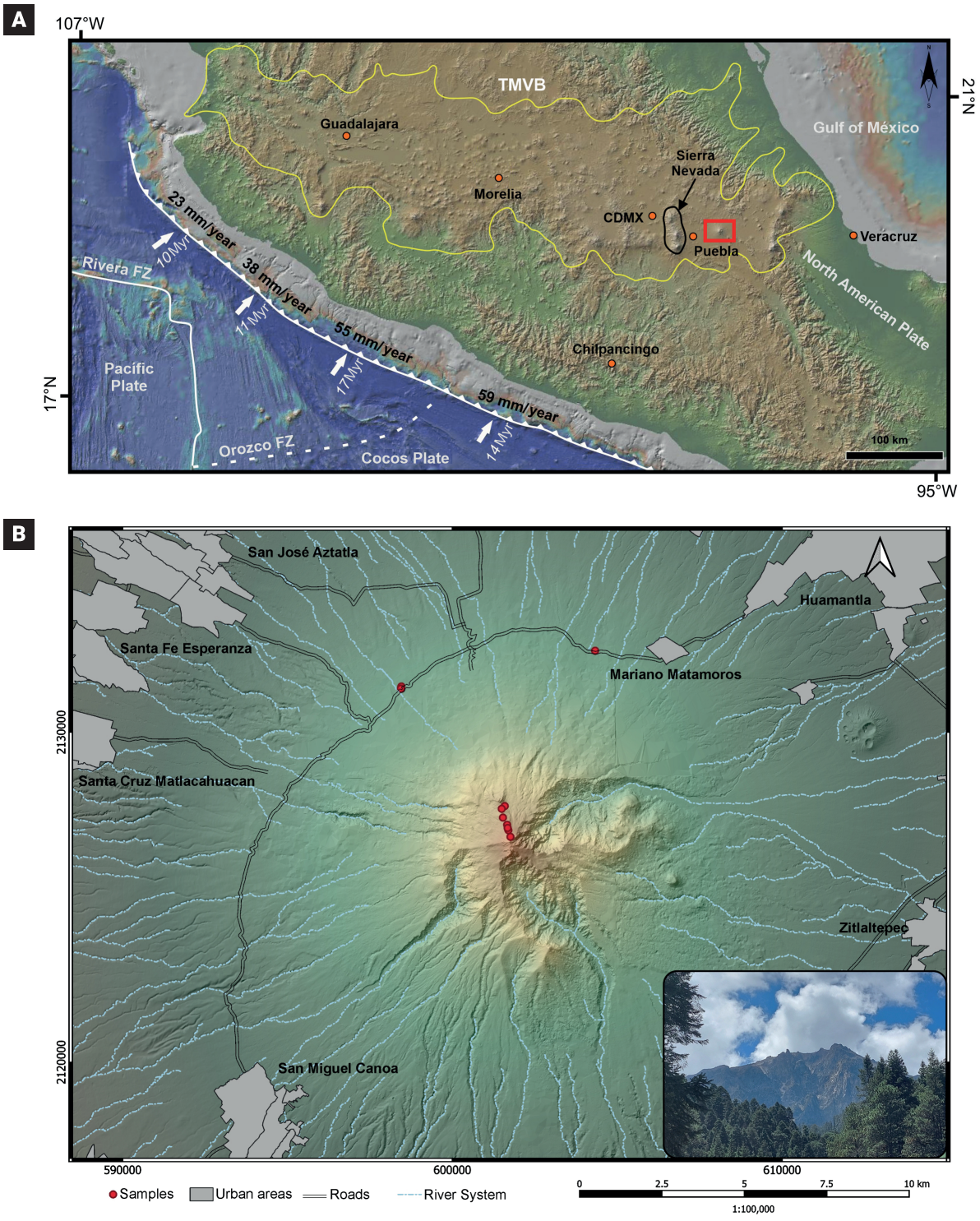

Figure 1. Location maps of the area. (A) Regional tectonic map of the central part of the Mexican territory. The continuous yellow line represents the Trans-Mexican Volcanic Belt (TMVB), the orange dots represent the main cities (CDMX: Mexico City), and the red box represents the study area. The black arrow points to the Sierra Nevada, which is located to the west of the La Malinche volcano and is formed by the Popocatépetl, Iztaccíhuatl and Tlaloc volcanoes. (B) Detailed map of the study area in La Malinche Volcano where the sampling sites are marked.

Castro-Govea (2007) and Castro-Govea and Siebe (2007) divided La Malinche's eruptive history into two main stages (Figure 2): Pre-Malinche and Malinche. The Malinche stage was further subdivided into three periods (Periods 1, 2, and 3) based on the characteristics of pyroclastic fall deposits: Huamantla Pumice, Malinche I Pumice, and Malinche II Pumice (Castro-Govea, 1999). According to Castro-Govea and Siebe (2007), Period 1 is marked by the oldest known pyroclastic deposit, Huamantla Pumice (>45 ka); Period 2 by the Malinche I Pumice (~21.4 ka); and Period 3 by the Malinche II Pumice (9–12 ka). Castro-Govea's (2007) work mainly emphasizes the volcano's eruptive chronology, providing a geological map of major deposit distributions, detailed petrographic and chemical characterizations of the volcanic products, and an in-depth study of a pyroclastic flow unit named the Upper Pilares Flow. The most recent investigation on La Malinche by Espinosa *et al.* (2021) explored the pre-eruptive conditions of the Malinche II Pumice. Their study documented textural evidence of disequilibrium and proposed magma mixing as a likely eruptive trigger. The presence of xenocrysts was also identified.

3. Geological Setting

La Malinche volcano is a large volcanic edifice with a basal diameter of approximately 28 km. Towards the summit, the structure loses its circular symmetry, presenting an elongated ridge instead, and notably lacks a summit crater. It belongs to the central-eastern sector of the Trans-Mexican Volcanic Belt (TMVB), which extends from the Pacific coastline to the state of Veracruz (Figure 1A). The formation of the TMVB is associated with the subduction of the Cocos Plate beneath the North American Plate along the Middle America Trench, generating typical calc-alkaline magmas (Mooser, 1972; Delgado-Granados, 1993; Besch *et al.*, 1995; García-Palomo *et al.*, 2002; Ferrari *et al.*, 2012).The precise nature of the basement underlying La Malinche remains uncertain, as eruptive deposits extensively cover the region.

However, the presence of limestone xenoliths in deposits from both La Malinche and the Sierra Nevada (e.g., Sosa-Ceballos *et al.*, 2012) suggests that the shallow basement likely consists of carbonate rocks (López-Ramos, 1979; Castro-Govea and Siebe, 2007). Likewise, in the region surrounding the volcano, Cretaceous calcareous units known as the Maltrata Formation crop out (López-Ramos, 1979; Castro-Govea and Siebe, 2007). Additionally, reef limestones with flint nodules (notably near Cerro Pinal; López-Ramos, 1979) and a tuff cone at Cerro Xalapaxco (Abrams and Siebe, 1994) suggest a sedimentary marine origin for the region's basement.

Structurally, three fault systems intersect beneath La Malinche: the NE-SW trending Malinche Fault, the NW-SE trending Hueyotlipan Fault, and the E-W oriented Tetlatlahuca Fault. Furthermore, regional structural lineaments trending N-S, NE-SW, NW-SE, and E-W have been documented (Castro-Govea and Siebe, 2007; Seele and Mooser, 1972).We present a reinterpretation of the geology of La Malinche, illustrated in Figure 3. The volcano is predominantly composed of the Malinche pyroclastic sequence (Ms), which includes pyroclastic flow deposits, pumice fall layers, and lahars, suggesting a diverse and complex eruptive history. Lava domes (Md) are concentrated around the summit, forming a main cluster with additional domes scattered along the slopes. These structures overlie older rocks from the Pre-Malinche volcanic stage (Pm), which are primarily dacitic with subordinate andesitic compositions. To the northeast, the Xalapaxco tuff cone (Xp) exhibits at least ten explosion craters with interbedded stratified surges and massive fall deposits. The region also contains volcanosedimentary (Vd) deposits consisting of alluvium, lahar deposits, breccias, and conglomerates. Collectively, La Malinche records a rich geological history, marked by complex eruptive behavior and geomorphological processes.

4. Methods

We collected pumice samples from three distinct Plinian deposits. Eleven pumice clasts were processed for mineral separation and subjected to petrographic and electron microprobe analyses (EPMA). Thin polished sections containing plagioclase phenocrysts were prepared to study melt inclusions. In addition, a bibliographic review was conducted to generate phase diagrams and infer pre-eruptive conditions, allowing comparison with our geothermobarometric data.

4.1. Modal analysis

Modal proportions in thin sections were determined through digital image analysis of whole-section photomicrographs taken at 4× magnification under polarized light. Crystal, vesicle, and glass boundaries were manually traced in CorelDRAW to create vector masks. These masks were subsequently analyzed in ImageJ v1.54 (Schneider *et al.*, 2012) using thresholding and particle analysis functions to calculate area percentages. This hybrid technique combined the precision of manual tracing with the reproducibility of digital analysis.

4.2. Fourier-Transform Infrared Spectroscopy of Melt Inclusions

A total of 141 melt inclusions hosted in plagioclase phenocrystals were extracted from pumice clasts belonging to Malinche I and Huamantla Pumice deposits.

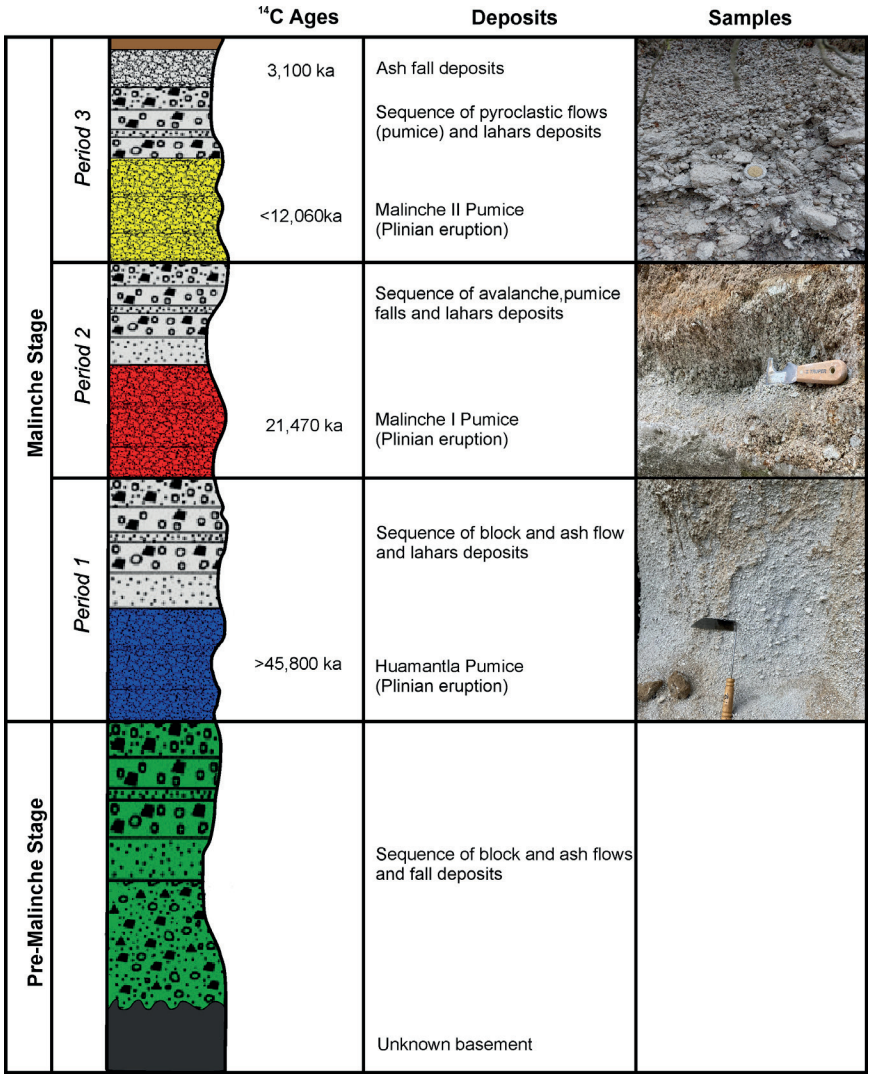

Figure 2. Composite stratigraphic section of La Malinche volcano. Modified from Castro-Govea, 2007. Not to scale.

Fourier-Transform Infrared Spectroscopy (FTIR) analyses were conducted to determine H_2O and CO_2 contents. We analyzed 123 inclusions in total, with 39 containing both H_2O and CO_2, and 74 containing only H_2O. FTIR analyses were carried out using a Thermo Scientific FT-IR Nicolet iS50 spectrometer (Microanalysis Laboratory, UNAM-IGUM). Liquid nitrogen was poured into the system two hours prior to analysis to cool the infrared detectors. Proper alignment of the IR light through the interferometer was verified before measurements. Spectra were processed using OMNIC Spectra software. Each spectrum was collected using 64 scans over a spectral range of 400–4000 cm^{-1} at a resolution of 4 cm^{-1}, with a 50×50 µm aperture. Volatile concentrations were calculated following the Beer-Lambert law as outlined by Befus *et al.* (2012). Inclusion thickness was measured under a microscope using the "z stage" method, focusing alternately on the upper and lower surfaces of each inclusion; measurements were repeated six times and averaged. Volatile data were then used to estimate saturation pressures and isobaric conditions employing the VolatileCalc software (Newman and Lowenstern, 2002; see Table 3)

4.3. Electron microprobe analysis

Eleven thin sections from Huamantla, Malinche I, and Malinche II Pumice deposits were analyzed. Mineral chemistry data were obtained for plagioclase, biotite, Fe-Ti oxides, and amphibole, as well as for glasses from melt inclusions and pumice groundmass (see **supplementary material 1**). Analyses were performed using a JEOL JXA-8600 electron microprobe (Microanalysis Laboratory, UNAM-IGUM). Analytical conditions included an accelerating voltage of 15 keV and a beam current of 10 nA for major elements, and 20 nA for selected trace elements. A focused beam was used for minerals, whereas a defocused beam (5 µm) was employed for groundmass glass to minimize

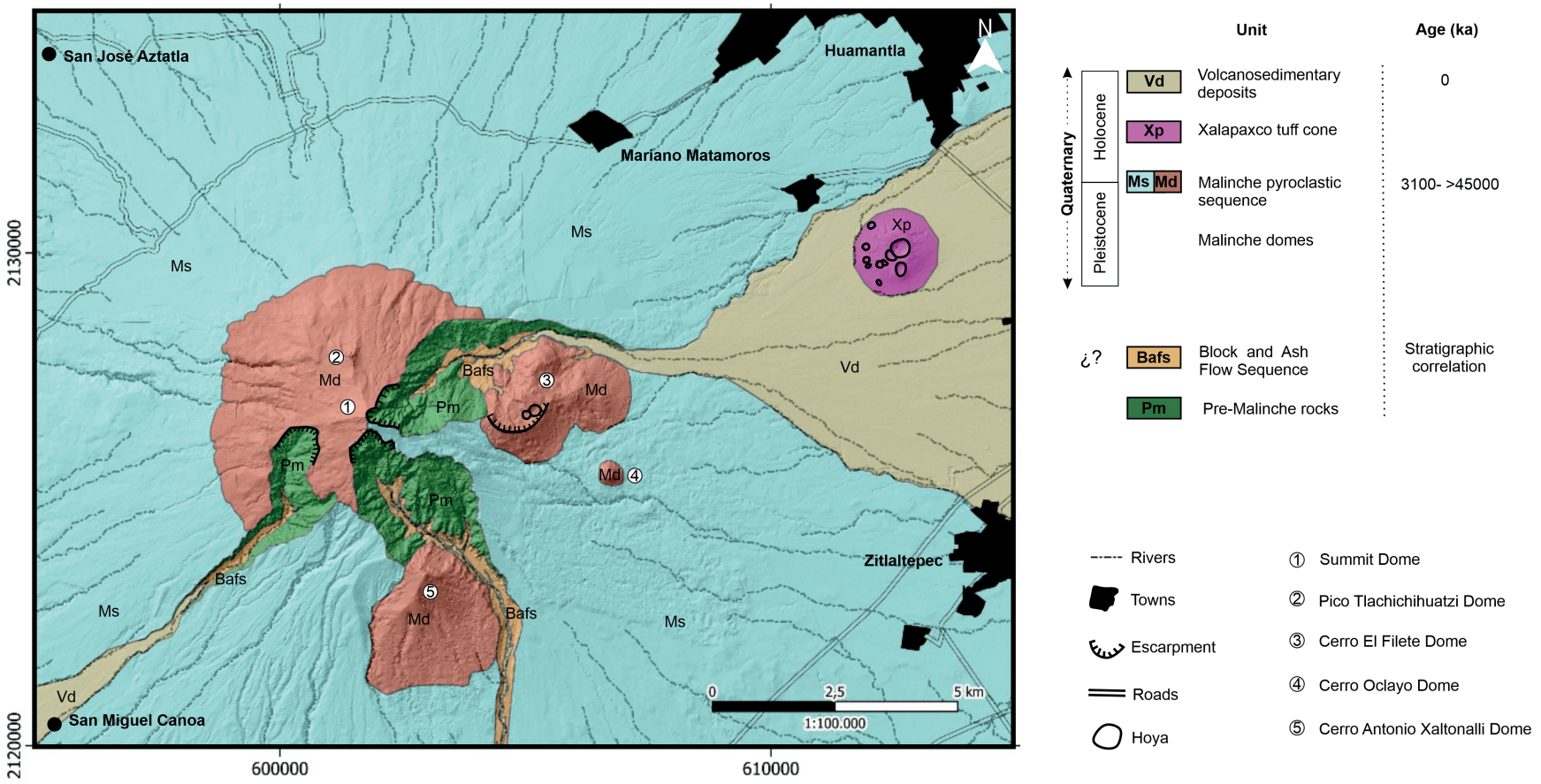

Vd Intercalation of alluvial deposits and lahar deposits made up of breccia and conglomerates interspersed with layers of finer material of ash and lapilli size, coming from La Malinche volcano.

Xp Xalapaxco tuff cone presents at least ten explosion craters that reveal alternating layers of stratified wave and massive fall deposits.

Ms Pyroclastic flows, pumice falls and lahar deposits, which indicate a varied and extensive eruptive cycle. It is part of the division made by Castro-Govea, (2007) which is made up of two main stages: Pre-Malinche and Malinche.

Md Complex structure with several lava domes. These domes are mainly concentrated in the summit area, forming a main group, although smaller domes also exist near the summit and on the slopes.

Bafs Pyroclastic deposits characterized by the mixture of volcanic rock fragments of various sizes, from blocks of more than one meter in diameter to fine ash.

Pm Rocks of an ancient volcanic edifice which show a variety of geomorphological and erosional characteristics that allow us to infer that they are much older with respect to other products. These rocks are mainly dacitic with variations to andesite.

Figure 3. Geological map of La Malinche volcano. The map legend is at the bottom and the delimited units and their chronology are shown at the top right. Hoya is a Spanish word meaning a depression on the earth's surface, similar to a caldera, but generally smaller.

alkali migration. Melt inclusion glasses were analyzed with a 10 μm defocused beam to reduce the effects of water loss and alkali migration. Analytical uncertainties were monitored and corrected using secondary standards and repeated measurements during each analytical session.

4.4. Bibliographic mineral stability line diagrams

Juvenile fragments from La Malinche show disequilibrium features and abundant xenocrysts (Castro-Govea, 2007; Espinosa *et al.*, 2021). Due to the xenocrystic nature of the samples, geothermobarometric results must be interpreted cautiously, and new experimental work to constrain pre-eruptive P–T conditions was avoided. To complement our geothermobarometry, we compiled experimental phase diagrams from representative silicic eruptions with ~75 wt. % SiO_2, including: the 1912 Novarupta eruption (Alaska, USA; Coombs and Gardner, 2001), the 1995–2002 Soufrière Hills eruptions (Montserrat; Rutherford and Devine, 2003), the Low-K rhyolites of Usu volcano (Japan; Tomiya *et al.*, 2010), the recent Cordón Caulle eruption (Chile; Castro *et al.*, 2013), and the Late Bishop Tuff (Long Valley Caldera, USA; Gardner *et al.*, 2014).

We selected the most evolved melt inclusions, hosted in euhedral plagioclase phenocrystals <1000 μm in size and free of disequilibrium textures, as proxies for the silica-rich melt that once dominated the reservoir. We assume that these rhyolitic melts reflect conditions prevailing within a relatively stationary reservoir, thereby justifying the application of published phase diagrams to infer the pre-eruptive conditions of La Malinche magmas.

5. Results

5.1. Petrography

Three distinct crystal size populations are identified: (1) microcrystals, defined in this study as crystals smaller than 300 μm; (2) phenocrystals, ranging from 300 μm to 1000 μm; and (3) megacrystals, with sizes between 10 and 30 mm.

Modal compositions are characterized by 10% crystals, 38% glass, and 52% vesicles for Huamantla Pumice; 15% crystals, 30% glass, and 55% vesicles for Malinche I Pumice; and 20% crystals, 20% glass, and 60% vesicles for the Malinche II Pumice. Modal analyses were carried out using ImageJ software (see Methods). The mineral assemblage in pumice from all three eruptions consists of plagioclase > amphibole > biotite > Fe-Ti oxides, with rare occurrences of quartz, which is present only in Huamantla Pumice. Notably, pyroxene is absent in all samples. The pumice exhibits a porphyritic texture. Plagioclase is the most abundant mineral phase in the samples, with an average grain size of 700 μm, and the smallest grains measuring less than 300 μm. Most crystals exhibit polysynthetic twinning and zoning. Some plagioclase phenocrystals display sieve textures toward their cores and rounded to irregular crystal edges (Figure 4A). Additionally, plagioclase glomerocrystals, plagioclase grains rimmed by amphibole (Figure 4C), and plagioclase crystals containing amphibole inclusions are also observed. Amphibole phenocrystals have an average size of ~500 μm and exhibit a tabular habit. They are commonly broken, display irregular edges, lack reaction rims, and contain oxide inclusions. Biotite phenocrystals also average ~500 μm in size and similarly show tabular habits, with some crystals fractured. Textural features observed in biotites include dissolution zones near the cores, inclusions of plagioclase and oxides, irregular edges, and occurrences within glomerocrystals. Iron and titanium oxide crystals range in size from <50 μm to 200 μm, with an average of ~100 μm. They display quadrangular, hexagonal, and rhombic habits. Fe-Ti oxides occur both as aggregates and as dispersed inclusions within other minerals. Quartz is rare, occurring as anhedral crystals up to 300 μm in size. Quartz grains exhibit rounded edges, are fractured, and commonly display irregular centers textures.

On the other hand, megacrystals in the pumice—defined as crystals larger than 1 mm—are predominantly plagioclase (up to 30 mm) and biotite (up to 28 mm), with amphibole also present (up to 23 mm) (Figure 4B). All megacrystals appear broken and exhibit evidence of dissolution and alteration, with characteristically rounded edges. Biotite contains inclusions of Fe-Ti oxides and plagioclase, while plagioclase hosts amphibole inclusions. Plagioclase also displays polysynthetic twinning, zoning, sieve textures toward the core, and exsolution textures (Figure 4D). Amphibole contains Fe-Ti oxide inclusions and shows irregular edges, whereas biotite exhibits irregular edges and dissolution zones near the core.

5.2. Mineral and glass chemical composition

Plagioclase compositions range from oligoclase to labradorite (Table 1, **Supplementary Material 1**), with overall An contents varying between An_{25} to An_{63}. Specifically, plagioclase in Huamantla Pumice ranges from An_{27} to An_{52}, in Malinche I Pumice from An_{25} to An_{63}, and in Malinche II Pumice from An_{26} to An_{56}. Average compositional zoning trends from rim to core vary slightly among the pumice types: An_{37} to An_{38} in Huamantla Pumice, An_{46} to An_{45} in Malinche I Pumice, and An_{45} to An_{36} in Malinche II Pumice (Figure 5A–B; Table 1, Supplementary Material 1), with overall An contents varying between An_{25} to An_{63}.

Specifically, plagioclase in Huamantla Pumice ranges from An_{27} to An_{52}, in Malinche I Pumice from An_{25} to An_{63}, and in Malinche II Pumice from An_{26} to An_{56}. Average compositional zoning trends from rim to core vary slightly among the pumice types: An_{37} to An_{38} in Huamantla Pumice, An_{46} to An_{45} in

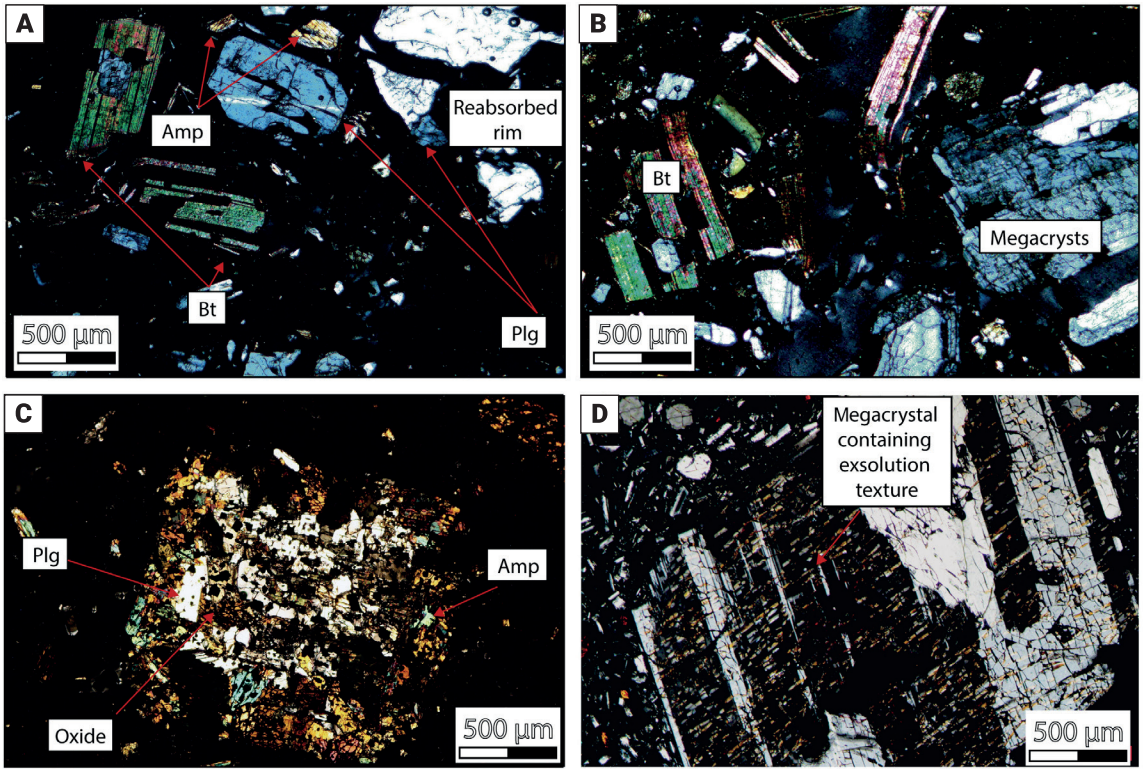

Figure 4. Photomicrographs of petrographic characteristics of Plinian eruptions of La Malinche Volcano. (A) Biotite, amphibole and plagioclase crystals of Huamantla Pumice; plagioclase present dissolution rims. (B) Biotite and plagioclase megacrystals of Malinche I Pumice. (C) Plagioclase with amphibole reaction rims of Malinche II Pumice. (D) Plagioclase megacrystal exhibiting exsolution texture and irregular edges. Amphibole (Amp), biotite (Bt), plagioclase (Plg).

Table 1. Summary table of the pre-eruptive conditions for plinian magmas of La Malinche volcano.

Eruption	Geothermobarometer type	Pressure (MPa)	Temperature (°C)	fO_2	H_2O content (wt. %)
Huamantla Pumice	Amphibole	308-74	910-775	-10.9 / -12.1	7.1-4.6
Malinche I Pumice	Amphibole	399-73	939-755	-10.1 / -12.8	7.3-4.5
Malinche II Pumice	Amphibole	420-143	946-820	-10.2 / -11.6	7.4-5.4
Huamantla Pumice	Fe-Ti oxides	-	928-885	-9.9 / -10.8	-
Malinche I Pumice	Fe-Ti oxides	-	934-835	-9.8 / -11.0	-

Malinche I Pumice, and An_{45} to An_{36} in Malinche II Pumice (Figure 5A–B). Amphibole is calcic in composition and corresponds to tremolite, pargasite, and magnesio-hornblende (Table 2, **Supplementary Material 1**). Both normal (i.e., decreasing Mg# toward the rim) and reverse (i.e., increasing Mg# toward the rim) zoning patterns are commonly observed in amphibole crystals (Figure 5D). Biotites from all three Plinian eruptions is classified as magnesio-biotite (Table 3, Supplementary Material 1). Biotite crystals display Mg# values ranging from 0.76 to 0.88, with Al contents between 1.22 and 1.44 (Table 3, Supplementary Material 1; Figure 5C). Fe-Ti oxides identified in Huamantla and Malinche I pumices include titanohematite and titanomagnetite (Table 4, Supplementary Material 1; Figure 5E). Glass matrix of the Plinian eruptions is mainly rhyolitic, but there are also dacitic compositions, varying from 65 to 76.4 wt.% in SiO_2 and alkalis from 3.2 to 7.3 wt.% (Table 5 in supplementary material; Figure 4F).

5.3. Geothermobarometers

Amphibole-based geothermobarometry was applied using the formulations of Ridolfi *et al.* (2010) for estimating fO_2, and

Table 2. Bibliographic summary table of the different compositions of major oxides in glass and plagioclase in magmas of rhyolitic composition.

Temperature range(°C)	Temperature Average (°C)	Pressure range (MPa)	Pressure Average (MPa)	Glass composition average									Plagioclase composition average								An content
				SiO_2	TiO_2	Al_2O_3	FeO	MnO	MgO	CaO	Na_2O	K_2O	SiO_2	TiO_2	Al_2O_3	FeO	MnO	MgO	CaO	Na_2O	K_2O	
650-700	675	0-100	50	-	-	-	-	-	-	-	-	-	-	-	-	-	-	-	-	-	-	-
650-700	675	100-200	150	71.42	0.31	8.16	6.73	0.01	0.24	0.17	6.17	4.44	-	-	-	-	-	-	-	-	-	-
650-700	675	200-300	250	76.75	0.08	14.48	0.79	0.20	0.11	1.94	4.31	1.30	61.17	0.01	24.58	0.15	0.01	0.01	6.17	7.77	0.13	0.30
700-750	725	0-100	50	74.20	0.29	13.90	1.91	0.23	0.06	1.37	4.51	3.21	-	-	-	-	-	-	-	-	-	-
700-750	725	100-200	150	71.15	0.30	8.61	6.87	0.04	0.21	0.40	6.13	4.33	-	-	-	-	-	-	-	-	-	-
700-750	725	200-300	250	76.14	0.13	14.32	1.33	0.26	0.14	1.82	4.38	1.42	59.72	0.04	24.83	0.26	0.02	0.01	7.13	7.84	0.15	0.33
750-800	775	0-100	50	74.40	0.26	13.90	1.68	0.16	0.06	1.05	4.89	3.33	-	-	-	-	-	-	-	-	-	-
750-800	775	100-200	150	73.17	0.26	9.98	5.02	0.09	0.18	0.71	5.71	3.50	59.11	0.01	25.77	0.23	0.02	0.01	7.88	6.82	0.13	0.39
750-800	775	200-300	250	76.93	0.13	13.73	1.18	0.27	0.14	1.71	4.38	1.46	60.30	0.02	25.00	0.21	0.01	0.01	7.11	7.19	0.15	0.39
800-850	825	0-100	50	75.74	0.26	13.41	1.64	0.23	0.12	1.17	4.60	2.62	58.19	0.01	26.25	0.23	0.02	0.01	8.38	6.78	0.13	0.40
800-850	825	100-200	150	72.13	0.29	11.68	4.34	0.19	0.18	1.17	5.80	3.20	55.84	0.01	27.58	0.35	0.01	0.01	10.29	5.84	0.08	0.49
850-900	875	0-100	50	72.76	0.40	14.18	2.41	0.40	0.12	1.76	5.28	2.46	56.13	0.02	27.42	0.49	0.03	0.04	10.34	5.47	0.09	0.51
850-900	875	100-200	150	70.60	0.55	14.75	3.16	0.57	0.12	2.06	5.24	2.79	-	-	-	-	-	-	-	-	-	-
900-950	925	0-100	50	70.00	0.65	14.35	3.52	0.61	0.12	2.06	5.66	2.81	-	-	-	-	-	-	-	-	-	-
900-950	925	100-200	150	-	-	-	-	-	-	-	-	-	-	-	-	-	-	-	-	-	-	-

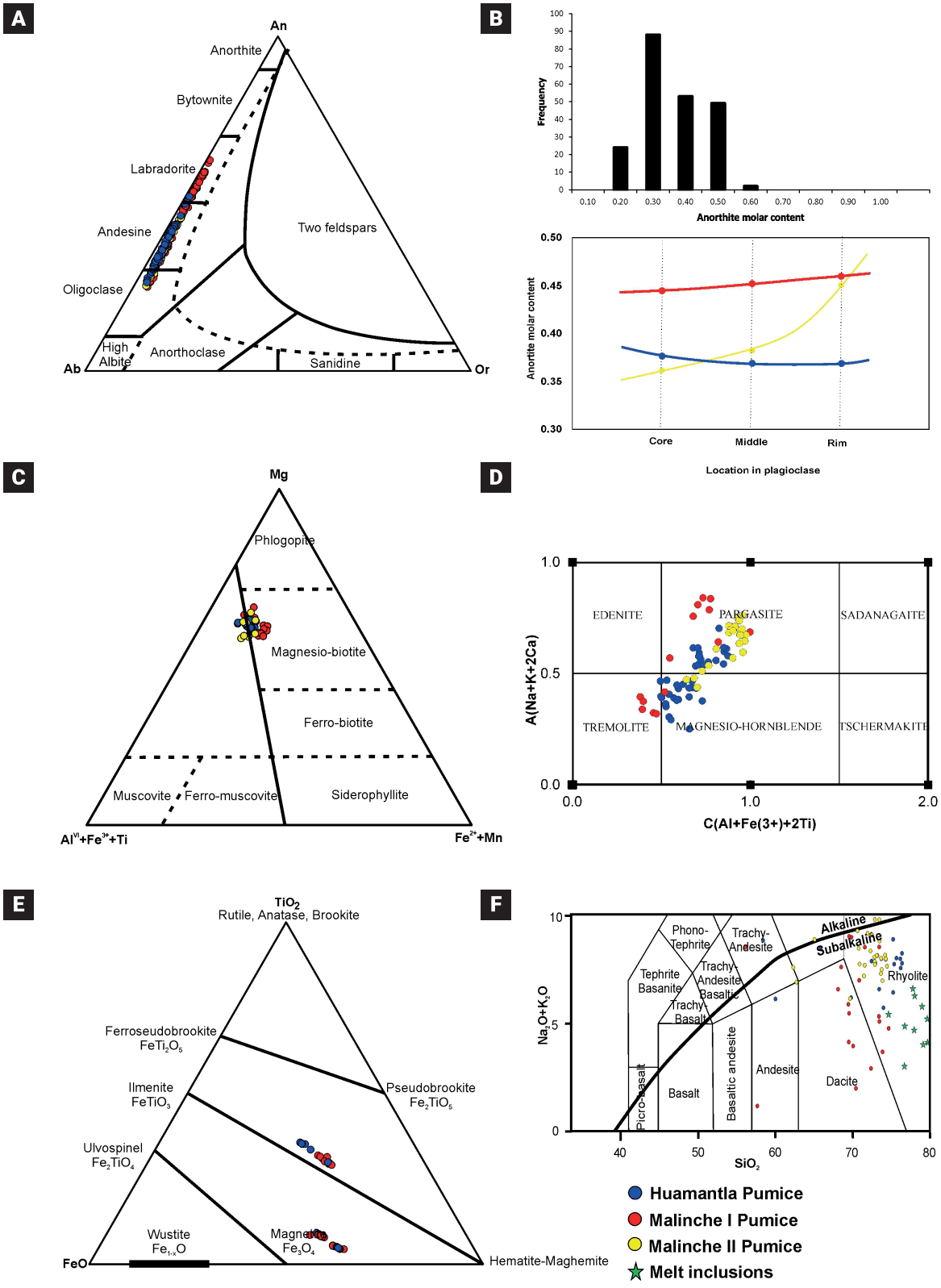

Figure 5. Mineral classification diagrams. (A) Plagioclase (Deer *et al.*, 1992). (B) Histogram of frequency in the molar content of An for the eruptions of the La Malinche volcano and average compositional variations in the plagioclase of each eruption from the core to the rim. (C) Biotite mineral classification diagram (Foster, 1960) (D) Amphibole mineral classification diagram (Hawthorne *et al.*, 2012). (E) Fe-Ti Oxides mineral classification diagram (Buddington and Lindsley 1964). (F) Classification diagrams using the composition of glass matrix from La Malinche volcano. TAS classification diagram (total alkali vs silica according to Irvine and Baragar, 1971) of the major element data normalized to 100%, on an anhydrous basis. It is possible to observe the wide compositional ranges that plagioclase and amphiboles have, unlike biotites, which are relatively more homogeneous than other minerals. The glasses, for their part, have a very wide compositional range.

Table 3. Summary table of the pressures calculated in VolatileCalc.

Eruption	H_2O (w.t %)	CO_2 (ppm)	Pressure (MPa)	H_2O (vmol%)	CO_2 (vmol%)
Huamantla	4.44	2275	382	17.7	82.3
Malinche I	0.82	4358	604	0.5	99.5
Malinche I	4.02	3282	544	18.3	81.7
Malinche I	2.46	4623	670	7.0	93.0
Malinche I	1.11	656	101	10.5	89.5
Malinche I	2.35	8888	1150	2.5	97.5
Malinche I	1.31	4519	634	2.7	97.3
Malinche I	4.60	5878	881	14.3	85.7
Malinche I	5.21	785	424	75.5	24.4
Malinche I	5.34	3116	737	46.7	53.3

Table 4. Summary table of the pre-eruptive conditions La Malinche volcano with all proxies.

Amphibole		Fe-Ti Oxides	Melt inclusions	Literature phase diagrams	
Pressure (MPa)	Temperature(°C)	Temperature(°C)	Pressure (MPa)	Pressure (MPa)	Temperature(°C)
150±50	800±10	895 ± 36	240±30	220	780

Ridolfi and Renzulli (2012) for temperature (T), pressure (P), and H_2O content (Table 6, **Supplementary Material 1**). A total of 81 analyses were evaluated, yielding crystallization conditions ranging from 946 to 755 °C and 420 to 73 MPa. Estimated melt H_2O contents vary from 7.4 to 4.5 wt.%, while log fO_2 values range between −10.1 and −12.8. Detailed results for each eruption are provided in Table 1 and illustrated in Figure 6A–C.

Fe–Ti oxide compositions were used to estimate temperature and oxygen fugacity (fO_2) using the geothermobarometer of Andersen and Lindsley (1985), implemented via the ILMAT Excel worksheet (Lepage, 2003; Table 7, Supplementary Material 1). Equilibrium between ilmenite and magnetite pairs was assessed following the criteria of Bacon and Hirschman (1988). For mineral pairs that passed the equilibrium test, calculated crystallization conditions range from 934 to 835 °C and log fO_2 values from −9.8 to −11.0 (Table 1; Figure 6A–C).

5.4. Melt Inclusions

The shapes of melt inclusions in plagioclase range from rounded to semi-rectangular (Figure 7A). Their sizes vary between 15 µm and >80 µm. Two-phase melt inclusions, consisting of glass and a vapor bubble, were observed; however, single-phase inclusions are more common in the samples (Figure 7C). Most inclusions are colorless, with a few showing greenish or brown hues (Figure 7B and 7D). Melt inclusions in Huamantla Pumice exhibit a narrow range of SiO_2 contents (~78.01 wt.%) and alkali contents of ~6.9 wt.% (Table 8, Supplementary Material 1).In contrast, melt inclusions in Malinche I Pumice, have a wider compositional range, with SiO_2 varying from 74.8 to 79.8 wt.% and total alkali content ranging from 3.6 to 6.5 wt. %. Overall, the average H_2O content in melt inclusions from the Plinian eruptions of La Malinche volcano is 2.9 wt.%, with values ranging from 0.29 to 7.76 wt.%. In Huamantla Pumice, the average H_2O content is 2.6 wt.%, within a range of 0.30 to 7.24 wt.%. For Malinche I Pumice, the average is 4.0 wt.%, with a range from 0.29 to 7.76 wt.% (Table 9, Supplementary Material 1).

5.5. Mineral stability lines diagrams modelling

Disequilibrium has previously been reported in rocks from La Malinche volcano, primarily based on textural evidence in mineral phases and the coexistence of multiple crystal populations formed under different pressure–temperature conditions (Castro-Govea and Siebe, 2007; Espinosa *et al.*, 2021). To better constrain the pre-eruptive conditions, we also draw upon studies from other volcanoes with similar mineralogical and geochemical characteristics, such as Popocatépetl, Cordon Caulle, the Novarupta eruption, the Late Bishop Tuff, and Usu volcano. We examined a series of experimental mineral stability diagrams produced for rocks with compositions matching that of the most evolved melt inclusions (>70 wt.% SiO_2) found in La Malinche phenocrystals. Based on this, we compiled a summary diagram highlighting the stability lines of mineral phases under specific P–T conditions. We interpret the composition of these melt inclusions as representative of a melt that was once in equilibrium

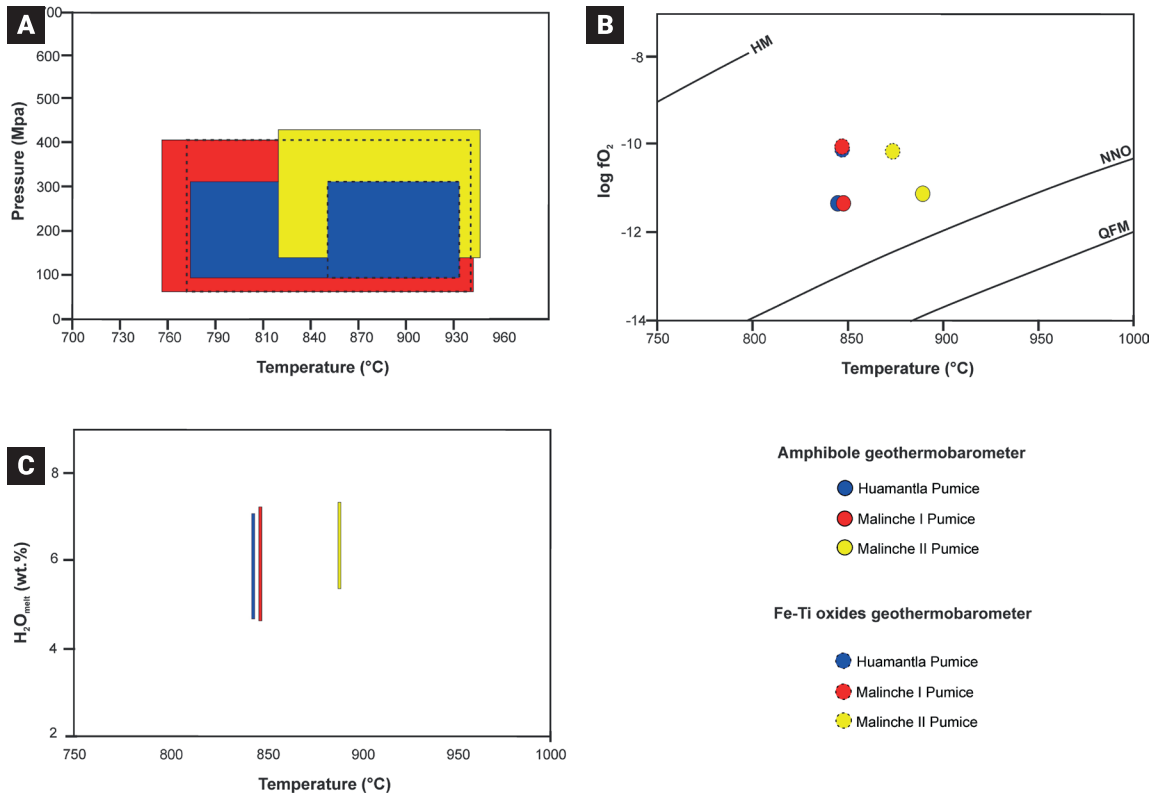

Figure 6. Crystallization conditions based on amphibole geothermobarometry (Ridolfi *et al.*, 2010; Ridolfi, and Renzulli, 2012) and Fe–Ti oxides geothermobarometry (Andersen and Lindsley, 1985) for the plinian eruptions of La Malinche volcano. (A) Temperature vs Pressure diagram. (B) Temperature vs log fO_2 diagram; the curves represent the magmatic buffers. (C) Temperature vs H_2O content diagram. It can be seen that the ranges are wide for each eruption, which suggests that they are not populations in equilibrium.

with the surrounding crystal assemblage, capturing a snapshot of magmatic equilibrium. Our goal is to approximate the pre-eruptive P–T conditions, likely within the range explored in laboratory experimental studies, and to further refine these estimates using additional methods such as geothermometry and volatile contents (H_2O–CO_2) in melt inclusions. In general, the mineral assemblage associated with high-silica compositions is defined by the stability lines of plagioclase, amphibole, biotite, quartz, pyroxene, potassium feldspar, and Fe–Ti oxides. The stability of these phases occurs within a pressure range of 50–200 MPa and temperatures between 700 and 950 °C (Figure 8A–B). Table 2 summarizes average compositions of glass and plagioclase (expressed in major oxides) under varying pressure and temperature conditions for rhyolitic magmas. The SiO_2 content in glass is highest at 700 °C and 250 MPa, and decreases at higher temperatures (e.g., 900 °C) and lower pressures (e.g., 150 MPa). In plagioclase, SiO_2 content is highest at 670 °C, decreasing at temperatures ≥825 °C and pressures around 150 MPa.

Based on this, we defined average mineral stability lines under different P–T conditions for rhyolitic magmas (Figure 8B). Plagioclase remains stable up to 950 °C and 220 MPa. Amphibole is stable between 760 and 860 °C and at pressures of 100–200 MPa. Biotite occurs within a narrower window, between 720 and 760 °C and 100–200 MPa. Quartz stability is restricted to 700–760 °C and pressures below ~190 MPa. Pyroxenes are stable at higher temperatures (>900 °C) and a broader pressure range (50–220 MPa). Potassium feldspar is stable between 730 and 770 °C at pressures of 170–200 MPa. Finally, Fe-Ti oxides are stable at temperatures above 950 °C and pressures exceeding 50 MPa.

6. Discussion

6.1. Magmatic processes below La Malinche volcano

Estimates of pre-eruptive conditions derived from laboratory experiments and geothermobarometric methods require chemical equilibrium within the magmatic system (Sisson *et al.*, 1989; Rutherford, 1993; Gardner *et al.*, 1995; Eskandari *et al.*, 2018; Pelullo *et al.*, 2022). However, due to the dynamic and heterogeneous nature of magma generation and evolution, achieving complete equilibrium is realistically unfeasible in most inter-

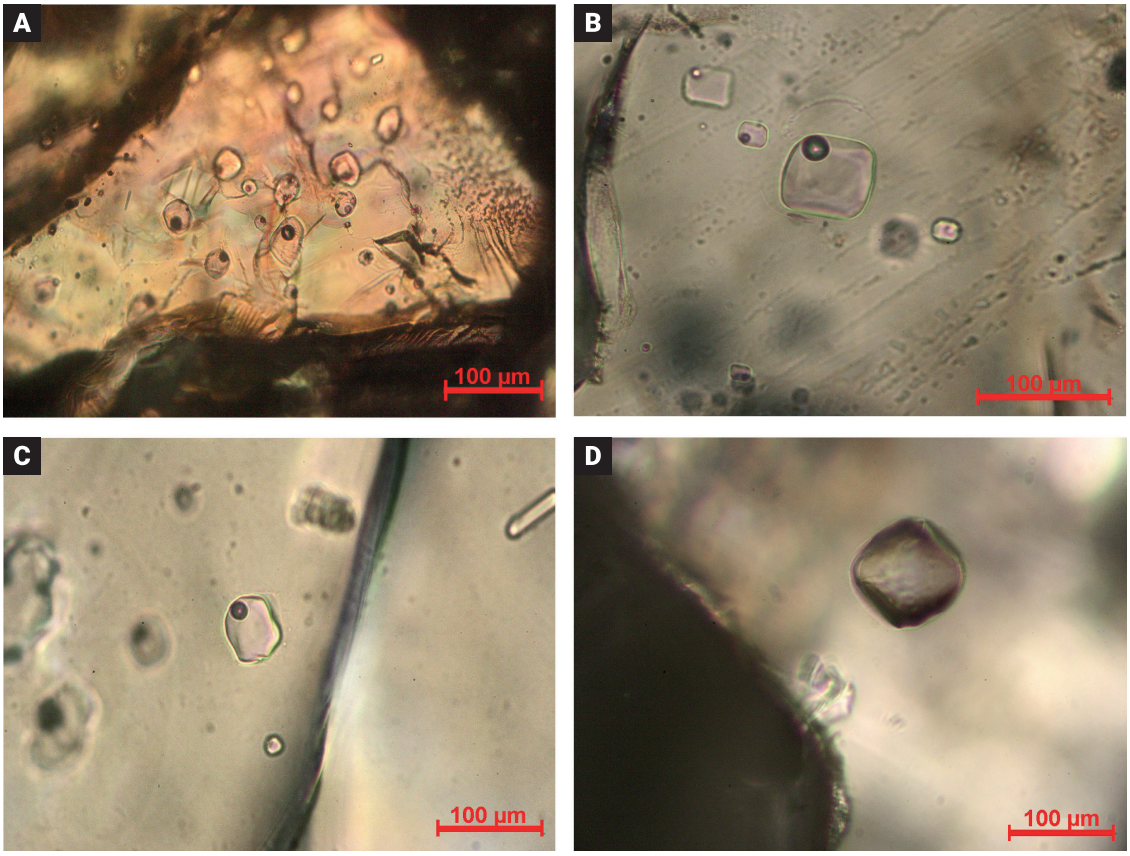

Figure 7. Photomicrographs of melt inclusions in the Plinian eruptions of La Malinche volcano. (A) Family of melt inclusions. (B) Melt inclusion of light coloration found in both eruptions. (C) Melt inclusions of different sizes and with bubbles. (D) Melt inclusion of dark coloration found in both eruptions. The compositions of the dark inclusions range from 66 to 71.5 SiO_2 wt. % and the compositions of the light inclusions range from 69 to 71.9 SiO_2 wt. %.

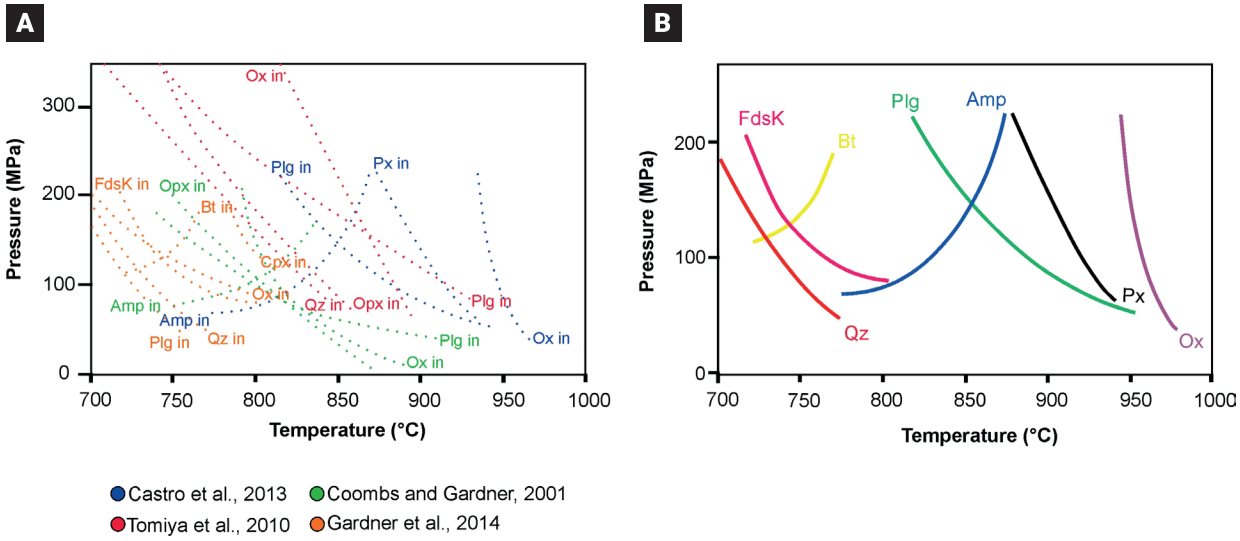

Figure 8. Mineral stability line diagrams obtained from bibliographic analysis on rhyolitic compositions. (A) Summary diagram for the rhyolitic composition in different works; shows the stability lines for amphibole (Amp), biotite (Bt), pyroxene (Px), oxides (Ox), plagioclase (Plg), potassium feldspar (FdsK)and quartz (Qz). (B) Diagram with the lines of average stability of the mineral phases present in magmas of rhyolitic composition.; shows the stability lines for amphibole (Amp), biotite (Bt), pyroxene (Px), oxides (Ox), plagioclase (Plg), potassium feldspar (FdsK)and quartz (Qz).

mediate magmas. According to experimental and geochemical studies, andesitic and dacitic magmas can evolve from basaltic parent magmas through differentiation processes such as crystal fractionation, assimilation, and magma mixing (Defant *et al.*, 1991). More recently, evidence has emerged showing that some dacitic and andesitic magmas in arc settings can also be directly derived from partial melting of the subducted lithosphere, particularly in settings where young, relatively hot oceanic crust is being subducted (Defant and Drummond, 1993; Drummond *et al.*, 1996). Determining the origin of andesites and dacites has long been a major objective in petrology, as these compositions dominate the eruptive output at convergent margins and closely match the average composition of the continental crust (Rudnick and Gao, 2003; Chiaradia *et al.*, 2011; Gill, 2012).

In continental arc volcanoes, eruptive products typically span a compositional continuum from basalt to dacite, and occasionally to rhyolite, following broadly linear trends (Hildreth *et al.*, 2003; Price *et al.*, 2005; Hora *et al.*, 2007; Singer *et al.*, 2008; Hildreth and Fierstein, 2012; Conway *et al.*, 2018). However, these compositional sequences are not always expressed in a temporally systematic manner, indicating that the fractional evolution of a long-lived magmatic reservoir is not consistently recorded in the eruptive history (Eichelberger *et al.*, 2006; Conway *et al.*, 2018).

In magma chambers beneath arc-related volcanic edifices, magmatic differentiation is primarily driven by crustal assimilation, magma mixing, and crystallization processes (Price *et al.*, 2012; Kent, 2013; Lee and Bachmann, 2014; Conway *et al.*, 2018). These processes can result in various evolutionary scenarios. One involves the accumulation of silicic magmas that are significantly more evolved than the bulk composition of the host rock (Reubi and Blundy, 2009; Kent, 2013; Conway *et al.*, 2018). Another is associated with disequilibrium textures that reflect the interaction between mafic and silicic magmas and their respective mineral assemblages, influenced by variations in pressure, temperature, and volatile content (Clynne, 1999; Dungan and Davidson, 2004; Kent *et al.*, 2010; Koleszar *et al.*, 2012; Conway *et al.*, 2018).

These processes are recorded in melt inclusions trapped in specific mineral phases and in interstitial glass (Reubi and Blundy, 2008), as well as in crystalline phases associated with intermediate magmatic compositions (Eichelberger, 1975; Streck *et al.*, 2007; Conway *et al.*, 2018). However, the scarcity of melt inclusions with intermediate compositions (Reubi and Blundy, 2009) has led to ongoing debate regarding how intermediate magmas attain equilibrium and how magmatic processes control their evolution. At La Malinche volcano, the influence of magma mixing —whether with more mafic magmas or via the incorporation of xenocrysts from the basement— is supported by binary plots of major and trace elements in pumice and lavas (see **Supplementary Material 2**).

Although research is ongoing to reconstruct the temporal evolution of La Malinche's magmatic system, our data suggest that compositional variability among pumice clasts from specific Plinian eruptions may reflect differences in groundmass composition or varying degrees of xenocryst incorporation. When pumice data are excluded, linear trends in whole-rock chemistry become more apparent, consistent with magma mixing and assimilation processes. Thus, to explore how magmatic processes may impact pre-eruptive condition estimates, we discuss the roles of magma mixing and assimilation during the Plinian eruptions of La Malinche volcano. It is important to emphasize that fractional crystallization is one of the key petrological processes in arc magmatic systems. Although often invoked as a major differentiation mechanism, once the melt cools sufficiently to allow mineral nucleation and growth, increasing viscosity hinders efficient crystal settling, thereby limiting the extent of crystal fractionation.

In this context, both the chemical and textural features of the Plinian deposits from La Malinche suggest that fractional crystallization was not the dominant process controlling the final composition of the erupted products. For example, the Huamantla Pumice —the oldest Plinian eruption— has a dacitic composition (>66 wt.% SiO_2; Castro-Govea and Siebe, 2007), indicating that a direct temporal progression from mafic to silicic compositions is not evident. This lack of systematic chemical evolution over time argues against simple fractional crystallization of a single parent magma.

Additional evidence comes from the zoning patterns in plagioclase phenocrysts. While average anorthite contents from core to rim show slight changes —Huamantla Pumice: $An_{37–36}$, Malinche I Pumice: $An_{45–46}$, and Malinche II Pumice: $An_{35–45}$ (Figure 4B)— the apparent homogeneity masks the broader compositional range of An_{60} to An_{20} observed in individual crystals. The relatively homogeneous averages in Huamantla and Malinche I contrast with the wider variability in Malinche II, possibly reflecting more complex thermal and compositional histories.

This pattern may imply that all three magma batches evolved within the same or similar magmatic reservoirs, but underwent distinct thermal regimes or degrees of open-system processes. Therefore, while fractional crystallization contributed to some degree of chemical differentiation, it was likely overprinted or accompanied by magma mixing, assimilation, and potentially recharge events. The textural features observed in plagioclase from the three Plinian eruptions of La Malinche—such as zoning, sieve textures in the core, and reaction rims—indicate thermodynamic disequilibrium, likely driven by mass addition or fluctuations in temperature, pressure, or oxygen fugacity (Bowen,

1937; Cox, 2013). These disequilibrium conditions reflect the influence of polybaric crystallization, which plays a key role in shaping the final composition of intermediate volcanic rocks (e.g., Cox, 2013; Marxer *et al.*, 2022).

6.1.1. Magma Mixing

Magma mixing is a petrological process that can occur both during the ascent of magma to the surface and, more commonly, within the magmatic reservoir (e.g., Anderson, 1976; Morgavi *et al.*, 2022). Evidence for mixing can be identified through disequilibrium textures in minerals (Couch *et al.*, 2001; Hazarika *et al.*, 2022), mixed populations of crystals (Cortés *et al.*, 2007), and variations in glass compositions observed in melt inclusions and groundmass (Kilgour *et al.*, 2013). One of the most recognized disequilibrium textures is sieve texture (Viccaro *et al.*, 2010; Yazdi *et al.*, 2019), which forms as a result of physical and chemical changes in the magmatic reservoir (Nelson and Montana, 1992; Stewart and Pearce, 2004). This texture typically arises from temperature fluctuations (Viccaro *et al.*, 2010; Yazdi *et al.*, 2019) or decompression under water-undersaturated conditions (Viccaro *et al.*, 2010; Yazdi *et al.*, 2019). In plagioclase crystals from La Malinche volcano, sieve textures are observed primarily in the cores of the crystals. These disequilibrium textures are likely linked to temperature variations caused by magma mixing or heating events that affected the reservoir, without triggering eruptions. When a hotter, more primitive magma is injected into the host magma, crystals near the contact zone become unstable, and the resulting increase in temperature can lead to dissolution, sieve textures, and the development of oscillatory zoning (e.g., Tepley *et al.*, 1999; Andrews *et al.*, 2008; Jarvis *et al.*, 2021). Additional evidence supporting magma mixing during the Plinian eruptions at La Malinche includes the presence of distinct crystal populations of amphibole and plagioclase. Three amphibole types were identified based on variations in pressure, temperature, water content, depth, and SiO_2 concentrations: pargasite, magnesio-hornblende, and tremolite. Similarly, plagioclase crystals exhibit compositional diversity, ranging from labradorite to andesine and oligoclase (Figure 5A and B). These mineralogical variations reflect the coexistence of crystals formed under different physicochemical conditions, further supporting the involvement of magma mixing in the pre-eruptive evolution of the system. Amphibole crystals from La Malinche can be grouped based on their formation conditions, particularly pressure, temperature, and composition. Three main pressure regimes are represented: <100 MPa, 100–200 MPa, and >300 MPa (Figure 9A). Correspondingly, amphiboles also cluster by temperature: tremolites crystallized between 730–790 °C, magnesio-hornblendes between 790–810 °C, and pargasites between 810–980 °C (Figure 9B). A clear inverse relationship is observed between SiO_2 content and crystallization pressure—amphiboles from lower SiO_2 melts (~45 wt.%) crystallized at higher pressures (200–300 MPa), whereas those from more evolved, higher SiO_2 melts (>48 wt.%) formed at lower pressures (100–180 MPa; Figure 9A). These groupings are consistent with depth estimates based on amphibole compositions (e.g., Ridolfi *et al.*, 2010), identifying three depth intervals: 3–5 km (tremolites), 5–15 km (magnesio-hornblendes), and 7–10 km (pargasites; Figure 9D). While two main depth clusters can be recognized, integration with compositional data refines these into three distinct amphibole populations.

Although pressure estimates overlap within the 5–10 km depth range, the compositional characteristics of each amphibole group are distinct, supporting the interpretation of different origins. Two of these groups—representing the highest and lowest pressure-temperature conditions—are compositionally distinct from the intermediate group (magnesio-hornblendes), which likely formed under hybrid conditions involving variable degrees of magma mixing and partial melting. The pargasites, characterized by higher temperatures and pressures (Figure 9), are Mg-rich amphiboles typically associated with mafic magmas (Rutherford and Devine, 2003; Kiss *et al.*, 2014). Their presence suggests the injection of mafic crystals into the magma reservoir, reflecting interaction between mafic melts and evolved silicic magmas or silicic basement lithologies. The occurrence of magnesian amphiboles—particularly pargasites—in La Malinche products and in previous studies (e.g., Macías *et al.*, 2017) strongly supports the interpretation of mafic recharge and magma mixing. At Colima volcano, for example, this type of magma mixing has been identified as a key mechanism in triggering explosive andesitic–dacitic eruptions.

In contrast, tremolites—which crystallize under lower pressure and temperature conditions—may be linked to intrusive bodies surrounding the magmatic reservoir and may reflect some degree of metamorphism or hydrothermal alteration (see discussion below). In the case of plagioclase, crystal populations ranging from labradorite to andesine and oligoclase are present in all three Plinian eruptions of La Malinche volcano. An contents cluster around An_{30}, but crystals with compositions ranging from An_{20} to An_{60} are also observed. The presence of calcic plagioclase (e.g., An_{63}) in Plinian products suggests the input of more mafic magmas or extreme thermal events (e.g., Sosa-Ceballos *et al.*, 2014). Calcium-rich plagioclase crystals (e.g., An_{63}) likely represent phases close to equilibrium with a hybrid andesitic melt and are thus interpreted as originating from mafic magma inputs. In contrast, more sodic plagioclase (e.g., An_{25}) is likely associated with partial assimilation of felsic crustal material, as discussed below. Likewise, this evidence of mixing is reflected

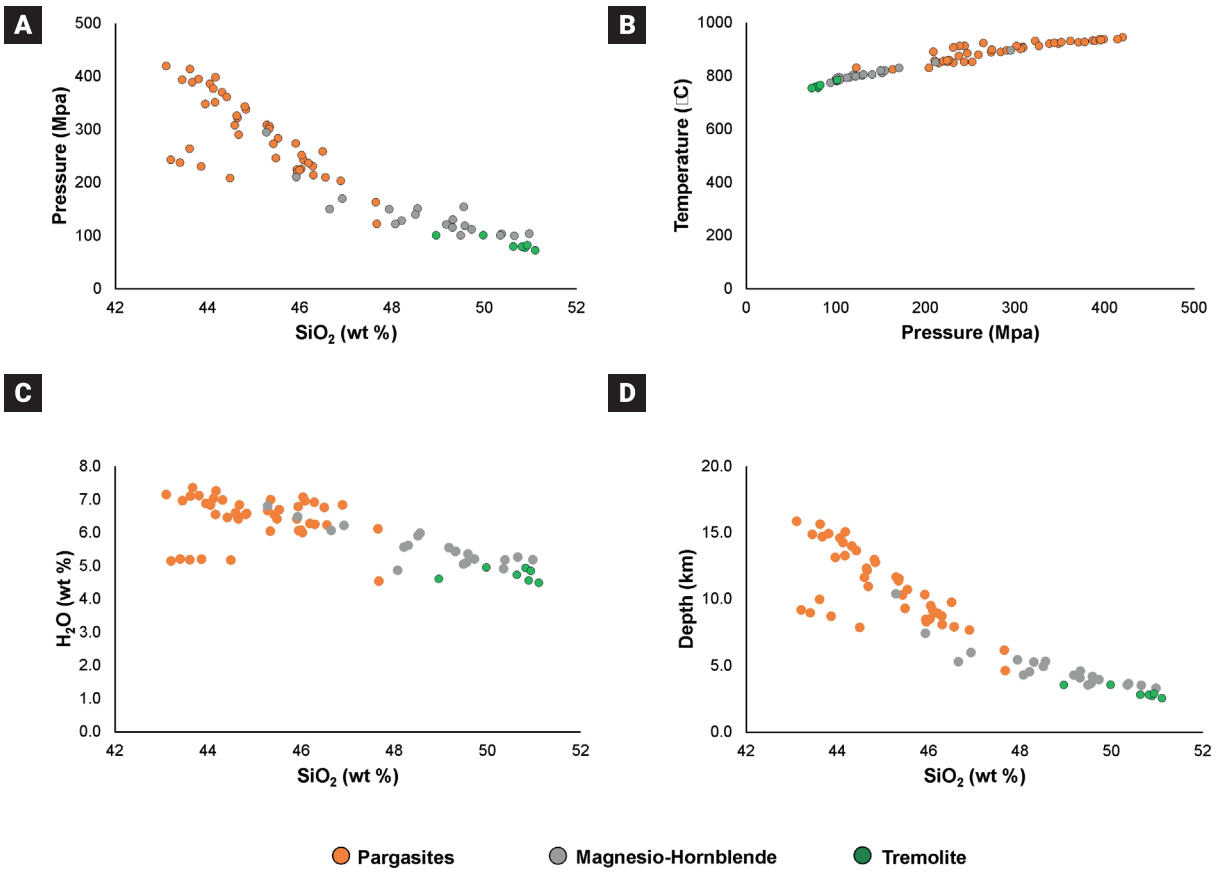

Figure 9. Diagrams showing the relationship of amphiboles populations with different physicochemical parameters. (A) Pressure vs SiO_2 content. (B) Temperature vs Pressure. (C) H_2O content vs SiO_2 content. (D) Depth vs SiO_2 content.

in the compositions of the glasses, which range from dacitic to rhyolitic. If the composition of the pumice groundmass glass is more evolved than the composition of the melt inclusions, this may indicate a dominant crystallization process.

Conversely, if the glass in pumice is less evolved than the melt inclusions, this may suggest that magma mixing was a frequent process and potentially acted as a trigger for eruption. It could also reflect the entrapment of early-formed phenocrysts (antecrystals) derived from the same magmatic batch. The glassy matrix of the Plinian eruptions from La Malinche volcano is predominantly rhyolitic, although dacitic compositions are also present, with SiO_2 contents ranging from 65.03 to 76.38 wt.% and total alkalis between 3.23 and 7.26 wt.%. In contrast, melt inclusions exhibit a narrower but more evolved compositional range, with SiO_2 from 74.8 to 79.8 wt.% and alkalis from 3.6 to 6.9 wt.%. This discrepancy supports the role of magma mixing in generating the observed compositional variability, particularly given that the melt inclusions generally reflect more evolved compositions (>75 wt.% SiO_2).Therefore, we propose that magma mixing at La Malinche volcano modified already evolved, polybarically crystallized melts by inducing changes in the physicochemical conditions of the magmatic reservoir. Similar mixing processes have been documented in other andesitic-dacitic stratovolcanoes (e.g., Schaaf *et al.*, 2005; Andrews *et al.*, 2008; Macías *et al.*, 2017). The injection of new magma increases both the volume and pressure of the reservoir, which can be inferred not only from compositional changes but also from the stability of specific mineral phases and the overall eruptibility of the system. Likewise, the thermal input from hotter magma injections would raise the reservoir's temperature, modifying mineral stability fields and potentially increasing the volatile content especially in amphibole- and biotite-bearing systems. It is important to note that it remains unclear whether these are isolated mixing events or recurrent processes throughout the volcano's history (e.g., Sosa-Ceballos *et al.*, 2014). If mixing events occur in a reservoir, the wall rocks may not only be assimilated or digested but also disaggregated and incorporated into the melt as fragments or crystal cumulates. Consequently, the melt composition would be altered through crustal assimilation.

6.1.2. Crustal Assimilation

Assimilation is a petrogenetic process capable of modifying magma composition during ascent or stagnation within the crust

(DePaolo, 1981; Best, 2003). Its occurrence can be inferred from the presence of xenocrystals and/or xenoliths, as well as through geochemical comparisons between the erupted products and the composition of the underlying crustal basement (Rollinson, 1993). In the case of La Malinche volcano, evidence for assimilation is primarily reflected in the size and composition of certain crystals within the mineral assemblage. One notable crystal population consists of megacrystals (>10 mm) of plagioclase, amphibole, biotite, and Ti-Fe oxides. These large crystals are readily identifiable in all three Plinian eruptions, both in hand samples and in thin section, and have also been documented in effusive products. A separate study is currently investigating the magmatic processes responsible for the final composition of La Malinche rocks and the relationship between its explosive and effusive products. The megacrystals exhibit rounded and irregular boundaries; in plagioclase megacrystals, sieve textures, compositional zoning, and exsolution features are common (Figure 4A). These characteristics suggest that the megacrystals are either xenocrystals or antecrystals. However, based on crystal textures and forthcoming geochemical analyses, they are most likely xenocrysts—incorporated into the magma from an external source. Many megacrystals display exsolution textures (Figure 4A), which are diagnostic of slow cooling in intrusive environments (Deer *et al.*, 1992; Best, 2003; Philpotts and Ague, 2009; Winter, 2014), thereby supporting their xenocrystic origin. Antecrystals display complex textures, including embayed or resorbed cores, which suggest partial dissolution under unstable physicochemical conditions such as fluctuations in temperature, magma composition, or pressure. These textures also include oscillatory zoning—indicative of compositional changes in the melt during crystal growth—and edge overgrowths that form when crystals, following dissolution episodes, regrow under more stable conditions. Such features are commonly associated with decompression events within the magmatic system, particularly during ascent from deeper storage regions. Under these conditions, crystals may experience rapid nucleation and growth, resulting in resorption textures, fluid inclusions from volatile exsolution, or zoned patterns that reflect dynamic pressure-temperature regimes (Davidson *et al.*, 2005; Zellmer *et al.*, 2008; Cooper and Kent, 2014).

Based on the available textural and geochemical evidence, the crystals analyzed in this study appear to be more consistent with a xenocrystic origin than with antecrystals. The presence of embayed cores, exsolution textures, and oscillatory zoning is more characteristic of crystals incorporated from external sources into the magmatic system. Nevertheless, the presence of antecrystals in La Malinche system cannot be definitively ruled out, and their occurrence remains a plausible component of the magmatic evolution. Regarding the chemical composition of the mineral assemblage, several key observations can be made. One group of amphiboles identified corresponds to tremolites. Tremolite commonly forms in intrusive bodies as a result of hydrothermal alteration of primary Fe-Mg silicates and may be linked to shallow-level intrusive environments (Stephenson, 1993; Cluzel *et al.*, 2020). It typically develops through the alteration of calcium- and magnesium-rich minerals, such as diopside or olivine, under metamorphic conditions. Additionally, metasomatic processes—where fluid-rock interactions lead to changes in rock chemistry—can also produce tremolite (Spear, 1993; Deer *et al.*, 1997; Klein and Dutrow, 2007). Second, the occurrence of plagioclase with albite-rich compositions has also been identified. These compositions are not typically expected in magmas with the whole-rock geochemistry observed in the eruptive products of La Malinche volcano, suggesting a possible contribution from felsic intrusive bodies. In certain granitic intrusions containing both plagioclase and amphibole (e.g., Oba, 1990; Papoutsa and Pe-Piper, 2014), similar mineral associations are observed, characterized by tremolitic amphiboles and albite-rich plagioclase. This mineralogical pairing, also present in the Plinian deposits of La Malinche, supports the hypothesis of assimilation of material from felsic intrusives during magma evolution. Finally, the presence of biotite with limited chemical variability across the three Plinian eruptions is particularly noteworthy, especially when contrasted with the compositional diversity observed among amphibole populations. One possibility is that biotite (specifically magnesian-biotite) crystallized during the late stages of magmatic differentiation in amphibole-bearing magmas (Speer, 1987; Underwood *et al.*, 2012). Alternatively, the biotite may be inherited from the local basement. Although xenoliths confirming this origin have not been identified, the evidence of magma mixing and the presence of xenocrystals in other mineral phases suggest that biotite should not be exempt from such processes. Therefore, we propose that some of the biotite crystals could have been assimilated from an unrecognized felsic basement.

Assimilation is capable of significantly modifying magma evolution. It can alter the liquidus and solidus temperatures of the system (e.g., Reiners *et al.*, 1995), disrupt crystallization sequences (e.g., Ghiorso and Kelemen, 1987), and induce substantial changes in the melt composition, particularly with respect to trace elements and isotopic signatures (Taylor, 1980; Reiners *et al.*, 1995). As a result, assimilation can shift a magma's evolutionary path and produce diverse rock types from the same parental melt (e.g., Kelemen and Ghiorso, 1986; Nielsen, 1988). Repeated injections of hot magma can supply the thermal energy necessary to partially melt the chamber walls and incorporate host rock material into the melt.

La Malinche volcano presents a unique case among nearby stratovolcanoes in the Sierra Nevada volcanic arc (e.g., Popocatépetl, Iztaccíhuatl, and Tlaloc), as it is characterized by an un-

usually high abundance of megacrystals. While Popocatépetl and Iztaccíhuatl have yielded xenoliths of granodioritic composition (Sosa-Ceballos *et al.*, 2012), La Malinche exhibits widespread megacrystic textures not only in its Plinian deposits but also in its effusive products, all of which are strongly porphyritic. Ongoing research is focused on the role of these megacrystals in eruptive dynamics and their potential tectonic controls.

6.2. Pre-eruptive conditions

6.2.1. Mineral stability diagrams

Mineral stability diagrams constructed from the available data delineate characteristic pressure–temperature intervals for minerals in magmatic systems analogous to those at La Malinche. However, it is evident that estimating phase equilibria becomes significantly more complex in magmas that have undergone substantial modification through assimilation and/or magma mixing—conditions well-documented in La Malinche system. Despite these complexities, the virtual stability lines diagrams provide valuable support for the pressure–temperature conditions independently calculated through mineral geothermobarometry and the analysis of melt inclusions (Figure 10A and 10B).

We propose that the most reliable approximation of the thermodynamic conditions that prevailed in the resident magma at a given time can be achieved through the analysis of melt inclusions as proxies. Melt inclusions with >78 wt.% SiO_2 are commonly enclosed in plagioclase crystals with silica contents around 62 wt.%. We interpret that melt inclusions hosted in phenocrystals (as opposed to megacrystals) record the effects of crustal assimilation or magma mixing processes that modified the magma composition prior to eruption. Following these processes, crystallization resumed and the magmatic reservoir likely remained at a relatively stable depth. Based on this, we consider the most evolved melt inclusions hosted in phenocrysts—those with >70 wt.% SiO_2—as representative of the melt accumulated in the reservoir. These inclusions serve as a valuable proxy for assessing pre-eruptive conditions through the use of rhyolitic phase diagrams, offering insights into the composition of the magma prior to further modification.

Plagioclase megacrystals are predominantly albitic, and the melt inclusions they host are expected to represent the most evolved compositions within the magmatic system. Importantly, only the inclusions with the highest silica contents were selected for analysis, while those showing evidence of post-entrapment water loss were excluded. Pressure estimates were obtained using VolatileCalc (Newman and Lowenstern, 2002), based on the volatile contents measured in the selected melt inclusions (see Table 3). Subsequently, a rhyolitic diagram was constructed using data from four previously published studies, incorporating rhyolitic compositions consistent with those identified in this work. The pink line was derived from experimental studies on rhyolitic compositions analogous to our melt inclusions. In these experiments, the stability conditions of glass and plagioclase were measured at specific pressures and temperatures. The resulting data (represented by pink points on P-T vs. SiO_2 content diagrams) were used to define a trend line, which reflects the compositional evolution. We acknowledge that this approach provides only an approximation and is not intended to yield precise values for pressure-temperature (P–T) conditions. However, it represents a valid and useful estimate for the magmatic system of La Malinche. The trend lines plotted in the diagram indicate comparable P-T conditions between rhyolitic compositions from published reference samples and the melt inclusions analyzed in this study. Furthermore, the virtual diagram developed here demonstrates high sensitivity, as variations in SiO_2 content reflect both compositional and thermodynamic conditions. For this reason, the mineral stability diagrams constructed in this work may also be applicable to other magmatic systems beyond La Malinche.

A careful selection of melt inclusions is essential to avoid the presence of xenocrystals, which could lead to misleading interpretations. Our results indicate that if an intermediate magma contains negligible xenocrystic content and crystal populations whose compositional variability arises solely from natural cooling processes, it is appropriate to conduct laboratory experiments. In the virtual diagram, a clear relationship emerges between the rhyolitic compositions of La Malinche melt inclusions and those from bibliographic sources, which were used to calibrate the rhyolitic trend line (Figure 10). By plotting the glassy groundmass compositions from each Plinian eruption alongside the melt inclusion compositions (Figs. 10A and B), we established a general trend line representing the P–T conditions of La Malinche magmas. Extrapolating the melt inclusion compositions onto this rhyolitic trend line allows us to infer the corresponding pressure and temperature conditions. This method yields estimates that are consistent with those obtained through other approaches, suggesting approximate conditions of 220 MPa and 780 °C for the magma reservoir.

6.2.2. Geothermobarometers

Geothermobarometry ideally reflects equilibrium conditions within a magma reservoir that is, the full range of pressure and temperature represented by the crystallized mineral assemblage. In the case of La Malinche volcano, equilibrium conditions are assessed primarily through amphibole and Fe-Ti oxide geothermobarometers. As previously discussed, three distinct compositional groups of amphiboles crystallized under different pressure–temperature (P–T) conditions, as evidenced in the Plinian eruptive products. Among them, magnesium hornblende

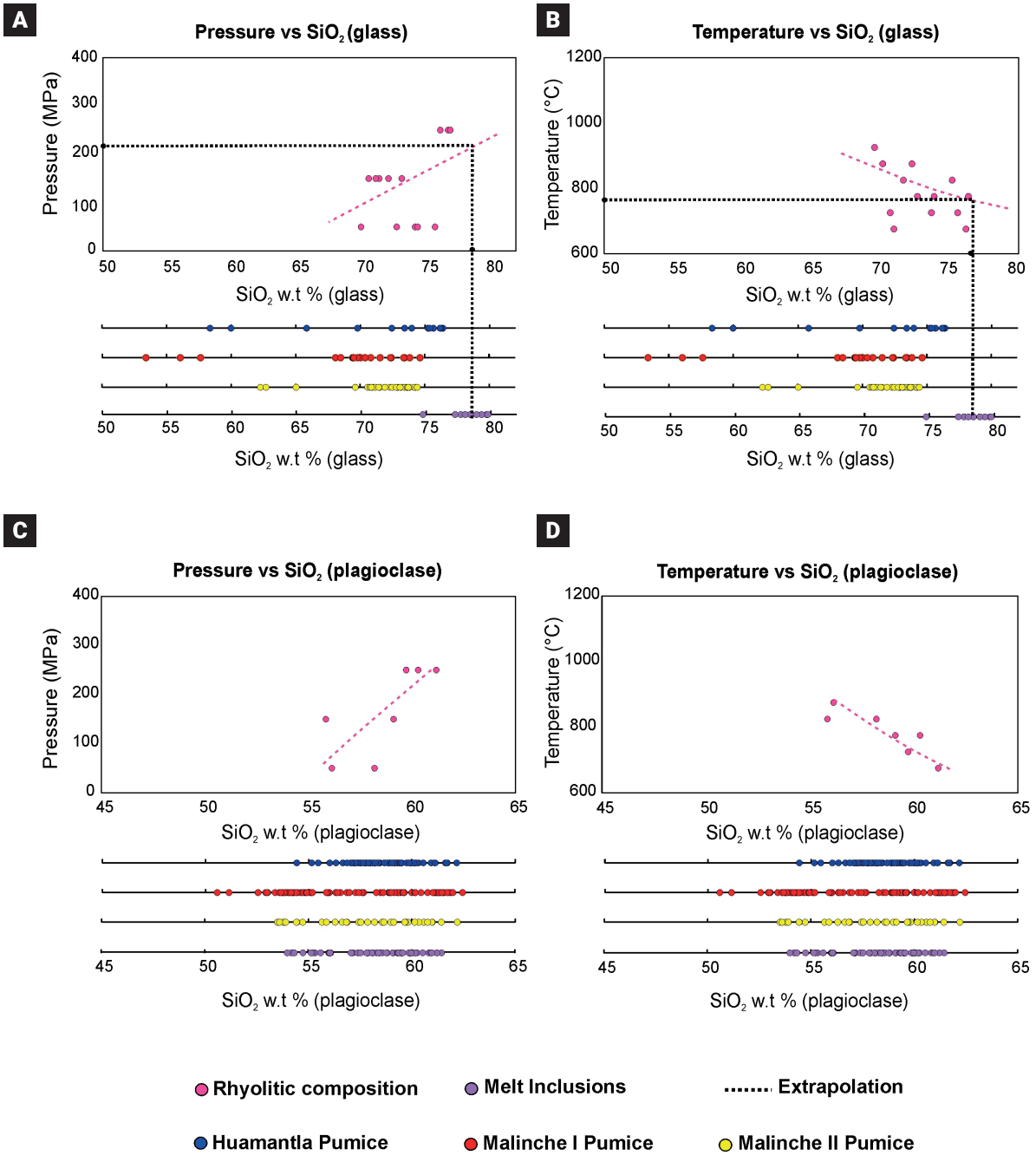

Figure 10. Pressure and temperature variation vs. SiO_2 content for glass and plagioclase in rhyolitic and andesitic compositions and plinian eruptions of La Malinche volcano. (A) Pressure vs SiO_2 content of glass (B) Temperature vs SiO_2 content of glass. (C) Pressure vs SiO_2 content of plagioclase. (D) Temperature vs SiO_2 content of plagioclase. It is important to recall that the most silica inclusion was used as an approximation; the trend resulting from the experimental variation was intersected and the value of the intersection with the train was projected to obtain the value of the variable on the "y" axis. The trend line for rhyolitic compositions (pink lines); plotting of the groundmass glass compositions for each Plinian eruption of the La Malinche volcano (blue, red and yellow color points), and the compositions of the melt inclusions (represented by the purple points).

appears to be the group most representative of equilibrium crystallization within the magma reservoir. These crystals formed under conditions of approximately 150 ± 50 MPa and 800 ± 10 °C. Therefore, these values are taken as reference conditions for the magma reservoir, representing average P–T estimates derived from amphibole-based geothermobarometry. For the Fe-Ti oxides, we applied the geothermobarometer of Andersen and Lindsley (1985) using the ILMAT Excel worksheet (Lepage, 2003) and tested equilibrium conditions through the coexistence of ilmenite and magnetite, following

the method of Bacon and Hirschmann (1988) (see **Supplementary Material 1**). The temperature calculated for the Fe-Ti oxides was not derived from Fe-Ti oxides megacrystals (which are indeed present in La Malinche samples), suggesting that these are not related to assimilation processes. The temperature obtained from the Fe-Ti oxides was 895 ± 36°C. Comparing this with the temperatures derived from the amphiboles and oxides, a consistent temperature of approximately 820 °C emerges, which likely reflects the equilibrium conditions of the magma reservoir.

6.2.3. Melt inclusions

Post-entrapment crystallization (PEC) is a common process in melt inclusions and is of significant importance due to the modifications it causes to glass composition and volatile content. We analyzed 10 melt inclusions for water and CO_2, ensuring that only crystal-clear inclusions were considered for glass composition determination. Although no crystals were observed petrographically, the Al_2O_2 content for a given SiO_2 in the glass suggested that some PEC had occurred. We assumed that all crystals originated from a single magmatic system, and that the glass analysis represents a mixture of PEC crystals and the surrounding melt. Our findings suggest that PEC contributes between 10 and 20% (**Supplementary Material 2**). The equilibrated compositions and volatile contents are presented in Tables 8 and 9 (Supplementary Material 1).

On the other hand, melt inclusion analyses are characterized by a sodium (Na) deficiency, with an average of 1.6 wt% Na_2O (Table 8 in Supplementary Material), when compared to the pumice matrix glass compositions. Na-deficient compositions in silicate-hosted melt inclusions have been previously reported, and Na concentrations can be modified in mineral-hosted melt inclusions after entrapment through diffusion of Na via the mineral (Audetat *et al.*, 2000; Audetat and Pettke, 2003; Zajacz *et al.*, 2008; Zajacz *et al.*, 2009). However, it should be considered that Na can be underestimated during electron probe analysis, as the use of an unfocused beam for water-rich compositions can lead to a relative loss of Na of up to 15-20%. This may explain the Na deficiency observed in the melt inclusions from La Malinche volcano. In Huamantla Pumice inclusions, the water content is 2.6 wt.%, with 1236 ppm of CO_2, indicating a trapping pressure of approximately 240±30 MPa, and the melt has a rhyolitic composition (78 wt.% SiO_2). The Malinche I Pumice contains 4.0 wt.% water and 895 ppm of CO_2, corresponding to a trapping pressure of approximately 207 MPa. The melt inclusions from this eruption also show a rhyolitic composition with high silica content (78.2 wt.% SiO_2). The saturation pressures of H_2O-CO_2 in the melt inclusions (240±30 MPa) and the pressures calculated from the amphiboles (150±50 MPa) in the Plinian eruptions of La Malinche volcano, along with their respective standard deviations, suggest a similarity between the two methods. This allows us to propose the presence of a single magma chamber from which these eruptions originated. However, it is important to note that since there is no evidence that the magma was completely saturated with liquid, the calculated pressures may be overestimated to some extent. Therefore, the values obtained should be interpreted with caution, considering the possibility of a lower real pressure in the magmatic system. To address this, the pressure values are correlated with the amphibole geobarometric methods and the virtual diagrams to constrain the pressure estimates.

6.2.4. Integrated pre-eruptive conditions

The combination of all the methods used provides an approximate range of pre-eruptive crystallization conditions for La Malinche magmas (Table 4). The Huamantla Pumice eruption occurred under pre-eruptive crystallization conditions at an average temperature of 866±50°C and pressures of 200±70 MPa. The Malinche Pumice I eruption had pre-eruptive conditions of 847±60°C at 222±30 MPa, while the Malinche II Pumice eruption occurred at slightly higher temperatures (880±60°C) and pressures of 280±90 MPa. Given the uncertainty in pressure estimates, it appears that all three Plinian eruptions of La Malinche originated from the same magma chamber at a consistent depth.

This observation has important implications for the evolution of magmas at La Malinche. The oldest eruption we studied (Huamantla Pumice, with >66% SiO_2) is the most evolved and may represent the initial stages of the reservoir's opening, corresponding to the explosive Plinian events. During this phase, assimilation of wall rock likely played a significant role. As time progressed, however, the eruptions became less evolved (Malinche II Pumice, the youngest, with SiO_2 content of 63%), suggesting that the magma chamber had become more stable. Magmas from this period were likely transient, with less interaction with the wall rocks, and may have been influenced by magmatic processes in deeper reservoirs.

This trend could also be tied to fractional crystallization and the volume of reinjected mafic magmas. Once a magma chamber was established, a series of magmas evolved over time through mixing, assimilation, and crystallization. These magmas were most likely never contemporaneous, meaning they did not coexist. Plinian eruptions likely occurred as leftover magma from previous events crystallized or remained liquid due to multiple injections of discrete mafic volumes. The frequent mafic in-

jections gradually built up new magma batches, and combined with assimilation and crystallization, these formed the magmas that erupted.

In this context, unlike the volcanoes Popocatépetl (Sosa-Ceballos *et al.*, 2014) and Iztaccíhuatl (Sosa-Ceballos G., personal communication), La Malinche volcano appears to have only one reservoir. However, further investigations on effusive deposits are needed to confirm this. Some of the reservoirs of the Sierra Nevada volcanoes are located at similar pressures and depths (Figure 11), with most of them grouped around 200 ± 50 MPa. According to Huber and Townsend (2019), this pressure range corresponds to the optimal rheological and structural conditions required for reservoirs to effectively hold eruptions and eventually release magma to the surface.

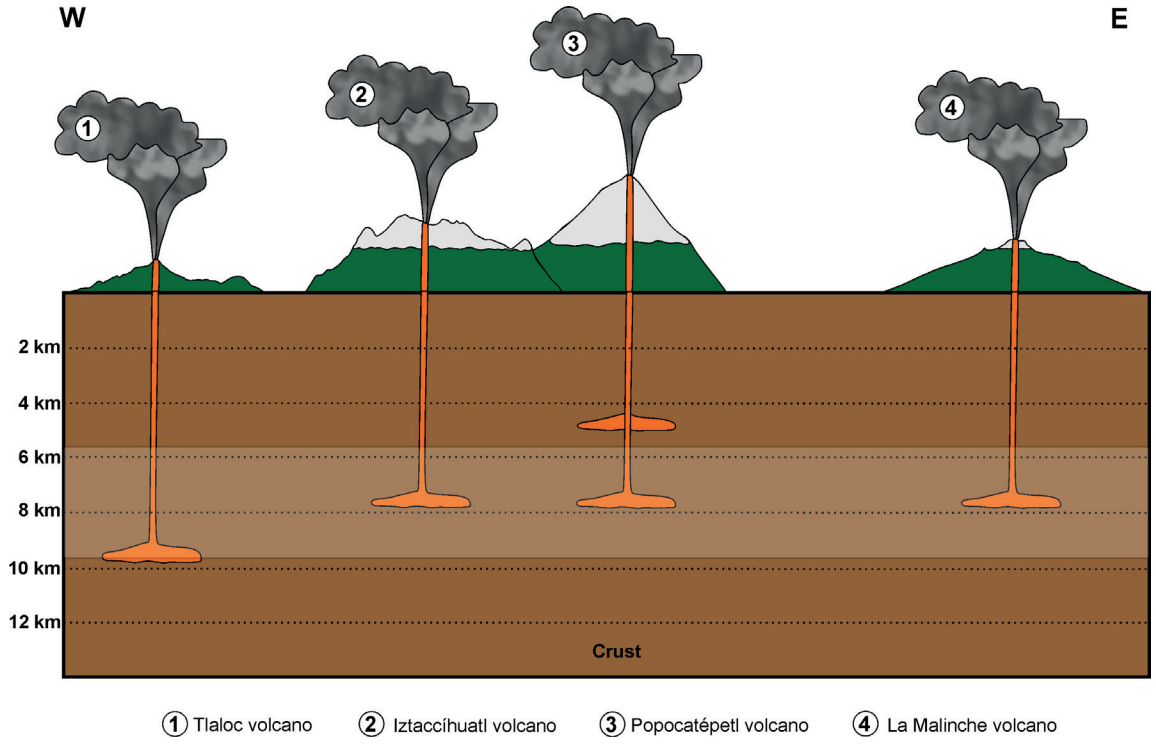

Figure 11. Representative model of the depth of the reservoirs of the Sierra Nevada volcanoes (Popocatépetl: Sosa-Ceballos *et al.*, 2021; 2014, Iztaccíhuatl: Sosa-Ceballos personal communication, and Tlaloc: Macias *et al.*, 2008, volcanoes) with respect to the reservoir of the La Malinche volcano. The storage area agrees with the observations of Huber and Townsend, 2019 (represented by a lighter band) which, through their interpretations, show that it is the depth at which magmas are stored in the crust

7. Conclusions

This research estimates the pre-eruptive conditions of La Malinche Volcano magmatic system, considering it is one of the largest active volcanoes in central Mexico, surrounded by approximately two million inhabitants within a 30 km radius. The mineral phases observed in the pyroclastic products include plagioclase (An_{20} to An_{60}), biotite (magnesium-biotite), amphiboles (magnesium-hornblende, pargasites, and tremolites), and Fe-Ti oxides (ilmenite and titanomagnetite). The presence of megacrystals of plagioclase, amphibole, and biotite suggests magmatic processes such as magma mixing and assimilation, indicated by the lack of equilibrium. We propose that magma mixing can enhance overpressurization and trigger eruptions in the La Malinche reservoir. The magmas that produced the Plinian eruptions of La Malinche were stored at approximately 200 ± 70 MPa and at a temperature of 820 ± 10°C. This corresponds to a reservoir depth of approximately 7.7 to 10.3 km, which is similar to the reservoir depths of volcanoes in the Sierra Nevada region.

8. Acknowledgments

This research was funded by DGAPA/PAPIIT-UNAM (IG100423) to Dr. Giovanni Sosa-Ceballos. We thank Dr. José Luis Arce, BSc. Delia González Preciado, BSc. Dahian Hernandez, MSc. Daniel Tapia and MSc. Gabriela Reyes for fieldwork support. We thank MSc. Daniel Tapia for his technical collaboration in GIS during the preparation of the preliminary geological map. The microprobe analysis was performed at the Microanalysis Laboratory, IGUM-UNAM, with the help of Dr. Noemí Salazar. The FTIR analyzes were carried out at the Microanalysis Laboratory, IGUM-UNAM, with the help of MSc. Gabriela Reyes. Preparation of thin sections and preparation of samples for chemistry were carried out at the IGUM-UNAM with the help of MSc. Felipe Garcia Tenorio and MSc. Fabiola Mendiola.

9. References

Abrams, M. J., & Siebe, C. (1994). Cerro Xalapaxco: an unusual tuff cone with multiple explosion craters, in central Mexico (Puebla). Journal of Volcanology and Geothermal Research, 63(3-4), 183-199. doi: **https://doi.org/10.1016/0377-0273(94)90073-6**

Andersen, D. J., & Lindsley, D. H. (1985). New (And Final) Models for the Ti- Magnetite/ilmenite Geothermobarometer and Oxygen Barometer. Eos Transactions American Geophysical Union, 66, 416.

Anderson, A. T. (1976). Magma mixing: petrological process and volcanological tool. Journal of Volcanology and Geothermal Research, 1(1), 3-33. doi: **https://doi.org/10.1016/0377-0273(76)90016-0**

Andrews, B. J., Gardner, J. E., & Housh, T. B. (2008). Repeated recharge, assimilation, and hybridization in magmas erupted from El Chichón as recorded by plagioclase and amphibole phenocrysts. Journal of Volcanology and Geothermal Research, 175(4), 415-426. doi: **https://doi.org/10.1016/j.jvolgeores.2008.02.017**

Arce, J. L., Gardner, J. E., & Macías, J. L. (2013). Pre-eruptive conditions of dacitic magma erupted during the 21.7 ka Plinian event at Nevado de Toluca volcano, Central Mexico. Journal of Volcanology and Geothermal Research, 249, 49-65. doi: **https://doi.org/10.1016/j.jvolgeores.2012.09.012**

Arzilli, F., La Spina, G., Burton, M. R., Polacci, M., Le Gall, N., Hartley, M. E., ... & Lee, P. D. (2019). Magma fragmentation in highly explosive basaltic eruptions induced by rapid crystallization. Nature Geoscience, 12(12), 1023-1028. doi: **https://doi.org/10.1038/s41561-019-0468-6**

Arzilli, F., Polacci, M., La Spina, G., Le Gall, N., Llewellin, E. W., Brooker, R. A., ... & Burton, M. R. (2022). Dendritic crystallization in hydrous basaltic magmas controls magma mobility within the Earth's crust. Nature Communications, 13(1), 3354. doi: **https://doi.org/10.1038/s41467-022-30890-8**

Audétat, A., & Pettke, T. (2003). The magmatic-hydrothermal evolution of two barren granites: A melt and fluid inclusion study of the Rito del Medio and Canada Pinabete plutons in northern New Mexico (USA). Geochimica et Cosmochimica Acta, 67(1), 97-121.

Audétat, A., Günther, D., & Heinrich, C. A. (2000). Causes for large-scale metal zonation around mineralized plutons: Fluid inclusion LA-ICP-MS evidence from the Mole Granite, Australia. Economic Geology, 95(8), 1563-1581. doi: **https://doi.org/10.2113/gsecongeo.95.8.1563**

Bacon, C. R., & Hirschmann, M. M. (1988). Mg/Mn partitioning as a test for equilibrium between coexisting Fe-Ti oxides. American Mineralogist, 73(1-2), 57-61. doi: **https://doi.org/10.1016/S0016-7037(02)01049-9**

Barberi, F., & Carapezza, M. L. (2019). Explosive volcanoes in the Mediterranean area: hazards from future eruptions at Vesuvius (Italy) and Santorini (Greece). Annals of Geophysics, 62(1), VO01. doi: **https://doi.org/10.4401/ag-7761**

Befus, K. S., Gardner, J. E., Zinke, R. W. (2012). Analyzing water contents in unexposed glass inclusions in quartz crystals. American Mineralogist, 97, (11-12), 1898-1904. doi: **https://doi.org/10.2138/am.2012.4206**

Besch, T., Verma, S. P., Kramm, U., Negendank, J. F. W., Tobschall, H. J., & Emmermann, R. (1995). Assimilation of sialic crustal material by volcanics of the easternmost extension of the Trans-Mexican Volcanic Belt Evidence from Sr and Nd isotopes. Geofísica Internacional, 34(3), 263–281. doi: **https://doi.org/10.22201/igeof.00167169p.1995.34.3.716**

Best, M. G. (2003). Igneous and Metamorphic Petrology (2a ed.). Malden: Blackwell.

Blatter, D. L., & Carmichael, I. S. (1998). Plagioclase-free andesites from Zitacuaro (Michoacan), Mexico: petrology and experimental constraints. Contributions to Mineralogy and Petrology, 132(2), 121-138. doi: **https://doi.org/10.1007/s004100050411**

Blatter, D. L., & Carmichael, I. S. (2001). Hydrous phase equilibria of a Mexican high-silica andesite: A candidate for a mantle origin?. Geochimica et Cosmochimica Acta, 65(21), 4043-4065. doi: **https://doi.org/10.1016/S0016-7037(01)00708-6**

Bonechi, B., Polacci, M., Arzilli, F., La Spina, G., Hazemann, J. L., Brooker, R. A., ... & Burton, M. R. (2024). Direct observation of degassing during decompression of basaltic magma. Science Advances, 10(33), eado2585. doi: **https://doi.org/10.1126/sciadv.ado2585**

Bowen, N. L. (1937). Recent high-temperature research on silicates and its significance in igneous geology. American Journal of Science, 5(193), 1-21.

Buddington, A. F., & Lindsley, D. H. (1964). Iron-titanium oxide minerals and synthetic equivalents. Journal of petrology, 5(2), 310-357. doi: **https://doi.org/10.1093/petrology/5.2.310**

Cassidy, M., Manga, M., Cashman, K., & Bachmann, O. (2018). Controls on explosive-effusive volcanic eruption styles. Nature communications, 9(1), 2839. doi: **https://doi.org/10.1038/s41467-018-05293-3**

Castillo-Rodríguez, M., López-Blanco, J., & Muñoz-Salinas, E. (2010). A geomorphologic GIS-multivariate analysis approach to delineate environmental units, a case study of La Malinche volcano (central México). Applied Geography, 30(4), 629-638. doi: **https://doi.org/10.1016/j.apgeog.2010.01.003**

Castro Govea, R. (2007). Historia eruptiva del volcán La Malinche y estudio del emplazamiento del flujo piroclástico Pilares Superior. [Tesis de doctorado], Universidad Nacional Autónoma de México, Ciudad de México.

Castro, J. M., Schipper, C. I., Mueller, S. P., Militzer, A. S., Amigo, A., Parejas, C. S., & Jacob, D. (2013). Storage and eruption of near-liquidus rhyolite magma at Cordón Caulle, Chile. Bulletin of Volcanology, 75(72), 1-17. doi: **https://doi.org/10.1007/s00445-013-0702-9**

Castro-Govea, R. (1999). Historia eruptiva reciente del volcán La Malinche. [Tesis de Maestría] Universidad Nacional Autónoma de México.

Castro-Govea, R., & Siebe, C. (2007). Late Pleistocene–Holocene stratigraphy and radiocarbon dating of La Malinche volcano, central Mexico. Journal of Volcanology and Geothermal Research, 162(1-2), 20-42. doi: **https://doi.org/10.1016/j.jvolgeores.2007.01.002**

Chiaradia, M., Müntener, O., & Beate, B. (2011). Enriched basaltic andesites from mid-crustal fractional crystallization, recharge, and assimilation (Pilavo Volcano, Western Cordillera of Ecuador). Journal of Petrology, 52(6), 1107-1141. doi: **https://doi.org/10.1093/petrology/egr020**

Cluzel, D., Boulvais, P., Iseppi, M., Lahondère, D., Lesimple, S., Maurizot, P., ... & Ulrich, M. (2020). Slab-derived origin of tremolite–antigorite veins in a supra-subduction ophiolite: the Peridotite Nappe (New Caledonia) as a case study. International Journal of Earth Sciences, 109, 171-196. doi: **https://doi.org/10.1007/s00531-019-01796-6**

Clynne, M. A. (1999). A complex magma mixing origin for rocks erupted in 1915, Lassen Peak, California. Journal of Petrology, 40(1), 105-132. doi: **https://doi.org/10.1093/petroj/40.1.105**

Conway, C., Gamble, J., Wilson, C., Leonard, G., Townsend, D. & Calvert, A. (2018). New petrological, geochemical, and geochronological perspectives on andesite-dacite magma genesis at Ruapehu volcano, New Zealand. American Mineralogist, 103(4), 565-581. doi: **https://doi.org/10.2138/am-2018-6199**

Coombs, M. L., & Gardner, J. E. (2001). Shallow-storage conditions for the rhyolite of the 1912 eruption at Novarupta, Alaska. Geology, 29(9), 775-778. doi: **https://doi.org/10.1130/0091-7613(2001)029<0775:SSCFTR>2.0.CO;2**

Cooper, K. M. (2019). Time scales and temperatures of crystal storage in magma reservoirs: implications for magma reservoir dynamics. Philosophical Transactions of the Royal Society A, 377(2139), 20180009. doi: **https://doi.org/10.1098/rsta.2018.0009**

Cooper, K. M., & Kent, A. J. R. (2014). Rapid remobilization of magmatic crystals kept in cold storage. Nature, 506(7489), 480-483. doi: **https://doi.org/10.1038/nature12991**

Cortés, J. A., Palma, J. L., & Wilson, M. (2007). Deciphering magma mixing: the application of cluster analysis to the mineral chemistry of crystal populations. Journal of Volcanology and Geothermal Research, 165(3-4), 163-188. doi: **https://doi.org/10.1016/j.jvolgeores.2007.05.018**

Couch, S., Sparks, R. S. J., & Carroll, M. R. (2001). Mineral disequilibrium in lavas explained by convective self-mixing in open magma chambers. Nature, 411(6841), 1037-1039. doi: **https://doi.org/10.1038/35082540**

Cox, K. G. (Ed.). (2013). The interpretation of igneous rocks. Springer Science & Business Media.

Davidson, J. P., Hora, J. M., Garrison, J. M., & Dungan, M. A. (2005). Crustal forensics in arc magmas. Journal of Volcanology and Geothermal Research, 140(1-3), 157-170. doi: **https://doi.org/10.1016/j.jvolgeores.2004.07.019**

Deer, W. A., Howie, R. A., and Zussman, J. (1992) An Introduction to the Rock-Forming Minerals. Longman, London

Defant, M. J., & Drummond, M. S. (1993). Mount St. Helens: potential example of the partial melting of the subducted lithosphere in a volcanic arc. Geology, 21(6), 547-550. doi: **https://doi.org/10.1130/0091-7613(1993)021<0547:MSHPEO>2.3.CO;2**

Defant, M. J., Richerson, P. M., De Boer, J. Z., Stewart, R. H., Maury, R. C., Bellon, H., ... & Jackson, T. E. (1991). Dacite genesis via both slab melting and differentiation: petrogenesis of La Yeguada volcanic complex, Panama. Journal of Petrology, 32(6), 1101-1142. doi: **https://doi.org/10.1093/petrology/32.6.1101**

Delgado Granados, H. (1993). Late Cenozoic tectonics offshore western Mexico and its relation to the structure and volcanic activity in the western Trans-Mexican Volcanic Belt. Geofísica Internacional, 32(4), 543–559. doi: **https://doi.org/10.22201/igeof.00167169p.1993.32.4.601**

Drummond, M. S., Defant, M. J., & Kepezhinskas, P. K. (1996). Petrogenesis of slab-derived trondhjemite–tonalite–dacite/adakite magmas. Earth and Environmental Science Transactions of the Royal Society of Edinburgh, 87(1-2), 205-215. doi: **https://doi.org/10.1017/S0263593300006611**

Dungan, M. A., & Davidson, J. (2004). Partial assimilative recycling of the mafic plutonic roots of arc volcanoes: An example from the Chilean Andes. Geology, 32(9), 773-776. doi: **https://doi.org/10.1130/G20735.1**

Eichelberger, J. C. (1975). Origin of andesite and dacite: evidence of mixing at Glass Mountain in California and at other circum-Pacific volcanoes. Geological Society of America Bulletin, 86(10), 1381-1391. doi: **https://doi.org/10.1130/0016-7606(1975)86<1381:OOAADE>2.0.CO;2**

Eichelberger, J. C., Izbekov, P. E., & Browne, B. L. (2006). Bulk chemical trends at arc volcanoes are not liquid lines of descent. Lithos, 87(1-2), 135-154. doi: **https://doi.org/10.1016/j.lithos.2005.05.006**

Eskandari, A., Amini, S., De Rosa, R., & Donato, P. (2018). Nature of the magma storage system beneath the Damavand volcano (N. Iran): An integrated study. Lithos, 300, 154-176. doi. **https://doi.org/10.1016/j.lithos.2017.12.002**

Espinosa, V. D., Arce, J. L., & Castro-Govea, R. (2021). Pre-eruptive conditions and reheating of dacitic magma (Malinche Pumice II Plinian eruption) at La Malinche volcano, Central Mexico. Journal of Volcanology and Geothermal Research, 419, 107368. doi: **https://doi.org/10.1016/j.jvolgeores.2021.107368**

Ferrari, L., Orozco-Esquivel, T., Manea, V., & Manea, M. (2012). The

dynamic history of the Trans-Mexican Volcanic Belt and the Mexico subduction zone. Tectonophysics, 522, 122-149. doi: **https://doi.org/10.1016/j.tecto.2011.09.018**

Foster, M. D. (1960). Interpretation of the composition of trioctahedral micas. US Geol. Surv. Prof. Pap., 354-B, 1-49.

García-Palomo, A. G., Macías, J. L., Tolson, G., Valdez, G., & Mora, J. C. (2002). Volcanic stratigraphy and geological evolution of the Apan region, east-central sector of the Trans-Mexican Volcanic Belt. Geofísica Internacional, 41(2), 133-150. doi: **https://doi.org/10.22201/igeof.00167169p.2002.41.2.282**

Gardner, J. E., Befus, K. S., Gualda, G. A., & Ghiorso, M. S. (2014). Experimental constraints on rhyolite-MELTS and the Late Bishop Tuff magma body. Contributions to Mineralogy and Petrology, 168, 1-14. doi: **https://doi.org/10.1007/BF00298703**

Gardner, J. E., Rutherford, M., Carey, S., & Sigurdsson, H. (1995). Experimental constraints on pre-eruptive water contents and changing magma storage prior to explosive eruptions of Mount St Helens volcano. Bulletin of Volcanology, 57(1), 1-17. doi: **https://doi.org/10.1007/BF00298703**

Ghiorso, M. S., & Kelemen, P. B. (1987). Evaluating reaction stoichiometry in magmatic systems evolving under generalized thermodynamic constraints: examples comparing isothermal and isenthalpic assimilation. En A. B.O. Mysen (Ed.) Magmatic Processes: Physicochemical Principles, (pp. 319-336). Geochemical Society

Gill, J. B. (2012). Orogenic andesites and plate tectonics (vol. 16). Springer Science & Business Media.

Ginibre, C., Wörner, G., & Kronz, A. (2007). Crystal zoning as an archive for magma evolution. Elements, 3(4), 261-266. doi: **https://doi.org/10.2113/gselements.3.4.261**

Goepfert, K., & Gardner, J. E. (2010). Influence of pre-eruptive storage conditions and volatile contents on explosive Plinian style eruptions of basic magma. Bulletin of Volcanology, 72, 511-521. doi: **https://doi.org/10.1007/s00445-010-0343-1**

Gualda, G. A., & Ghiorso, M. S. (2015). MELTS_Excel: A Microsoft Excel-based MELTS interface for research and teaching of magma properties and evolution. Geochemistry, Geophysics, Geosystems, 16(1), 315-324. doi: **https://doi.org/10.1002/2014GC005545**

Gurenko, A. A., Belousov, A. B., Trumbull, R. B., & Sobolev, A. V. (2005). Explosive basaltic volcanism of the Chikurachki Volcano (Kurile arc, Russia): Insights on pre-eruptive magmatic conditions and volatile budget revealed from phenocryst-hosted melt inclusions and groundmass glasses. Journal of Volcanology and Geothermal Research, 147(3-4), 203-232. doi: **https://doi.org/10.1016/j.jvolgeores.2005.04.002**

Hawthorne, F. C., Oberti, R., Harlow, G. E., Maresch, W. V., Martin, R. F., Schumacher, J. C., & Welch, M. D. (2012). Nomenclature of the amphibole supergroup. American Mineralogist, 97(11-12), 2031-2048. doi: **https://doi.org/10.2138/am.2012.4276**

Hazarika, G., Basumatary, P., Prakash, T., Chauhan, H., & Gogoi, B. (2022). Magma mixing dynamics in a vertically zoned granitic magma chamber inferred from feldspar disequilibrium assemblage and biotite composition: a case study from the Mikir Massif, eastern India. Acta Geochimica, 41(3), 453-469. doi: **https://doi.org/10.1007/s11631-022-00534-1**

Heine, K. (1971). Fechas 14C de los sedimentos del volcán La Malinche. Universidad Nacional Autónoma de México, Anuario de Geografía, 11, pp. 177-184.

Heine, K. (1984). The classical late Weichselian climatic fluctuations in Mexico. En C. C. N.-A. Mörner, W. Karlén (Eds). Climatic Changes on a Yearly to Millennial Basis: Geological, Historical and Instrumental Records (pp. 95-115). Dordrecht: Springer Netherlands.

Heine, K. (1988). Late Quaternary glacial chronology of the Mexican volcanoes. Geowissenschaften, 6, 197-205.

Heine, K., & Heide-Weise, H. (1973). Jungquartäre Förderfolgen des Malinche-Vulkans und des Popocatepetl (Sierra Nevada, Mexiko) und ihre Bedeutung für die Glazialgeologie, Paläoklimatologie und Archäologie. Münstersche Forschungen zur Geologie und Palaeontologie= Münster. Forsch. Geol. Paläont., 31, 303-322. doi: **https://doi.org/10.5283/epub.9606**

Hildreth, W., & Fierstein, J. (2012). Eruptive history of Mount Katmai, Alaska. Geosphere, 8(6), 1527-1567. doi: **https://doi.org/10.1130/GES00817.1**

Hildreth, W., Fierstein, J., & Lanphere, M. (2003). Eruptive history and geochronology of the Mount Baker volcanic field, Washington. Geological Society of America Bulletin, 115(6), 729-764. doi: **https://doi.org/10.1130/0016-7606(2003)115%3C0729:EHAGOT%3E2.0.CO;2**

Hora, J. M., Singer, B. S., & Wörner, G. (2007). Volcano evolution and eruptive flux on the thick crust of the Andean Central Volcanic Zone: 40Ar/39Ar constraints from Volcán Parinacota, Chile. Geological Society of America Bulletin, 119(3-4), 343-362. doi: **https://doi.org/10.1130/B25954.1**

Huber, C., Townsend, M., Degruyter, W., & Bachmann, O. (2019). Optimal depth of subvolcanic magma chamber growth controlled by volatiles and crust rheology. Nature Geoscience, 12(9), 762-768. doi: **https://doi.org/10.1038/s41561-019-0415-6**

Irvine, T. N., & Baragar, W. R. A. (1971). A guide to the chemical classification of the common volcanic rocks. Canadian journal of earth sciences, 8(5), 523-548. doi: **https://doi.org/10.1139/e71-055**

Jarvis, P. A., Pistone, M., Secretan, A., Blundy, J. D., Cashman, K. V., Mader, H. M., & Baumgartner, L. P. (2021). Crystal and volatile controls on the mixing and mingling of magmas. Crustal Magmatic System Evolution: Anatomy, Architecture, and Physico-Chemical Processes, 125-150. doi: **https://doi.org/10.1002/9781119564485.ch6**

Kelemen, P. B., & Ghiorso, M. S. (1986). Assimilation of peridotite in zoned calc-alkaline plutonic complexes: evidence from the Big Jim complex, Washington Cascades. Contributions to Mineralogy and Petrology, 94(1), 12-28. doi: **https://doi.org/10.1007/BF00371222**

Kent, A. J. (2013). Preferential eruption of andesitic magmas: Implications for volcanic magma fluxes at convergent margins. Geological Society, London, Special Publications, 385(1), 257-280. doi: **https://**

doi.org/10.1144/SP385.10

Kent, A. J., Darr, C., Koleszar, A. M., Salisbury, M. J., & Cooper, K. M. (2010). Preferential eruption of andesitic magmas through recharge filtering. Nature geoscience, 3(9), 631-636. doi: **https://doi.org/10.1038/ngeo924**

Kilgour, G., Blundy, J., Cashman, K., & Mader, H. M. (2013). Small volume andesite magmas and melt–mush interactions at Ruapehu, New Zealand: evidence from melt inclusions. Contributions to Mineralogy and Petrology, 166, 371-392. doi: **https://doi.org/10.1007/s00410-013-0880-7**

Kiss, B., Harangi, S., Ntaflos, T., Mason, P. R., & Pál-Molnár, E. (2014). Amphibole perspective to unravel pre-eruptive processes and conditions in volcanic plumbing systems beneath intermediate arc volcanoes: a case study from Ciomadul volcano (SE Carpathians). Contributions to Mineralogy and Petrology, 167, 1-27. doi: **https://doi.org/10.1007/s00410-014-0986-6**

Klein, C., & Dutrow, B. (2007). Manual de ciencias minerales . John Wiley e hijos.

Koleszar, A. M., Kent, A. J., Wallace, P. J., & Scott, W. E. (2012). Controls on long-term low explosivity at andesitic arc volcanoes: Insights from Mount Hood, Oregon. Journal of Volcanology and Geothermal Research, 219, 1-14. doi: **https://doi.org/10.1016/j.jvolgeores.2012.01.003**

La Spina, G., Arzilli, F., Burton, M. R., Polacci, M., & Clarke, A. B. (2022). Role of volatiles in highly explosive basaltic eruptions. Communications Earth & Environment, 3(1), 1-13. doi: **https://doi.org/10.1038/s43247-022-00479-6**

Lee, C. T. A., & Bachmann, O. (2014). How important is the role of crystal fractionation in making intermediate magmas? Insights from Zr and P systematics. Earth and Planetary Science Letters, 393, 266-274. doi: **https://doi.org/10.1016/j.epsl.2014.02.044**

Lepage, L. D. (2003). ILMAT: an excel worksheet for ilmenite-magnetite geothermometry and geobarometry. Computers & Geosciences, 29(5), 673-678. doi: **https://doi.org/10.1016/S0098-3004(03)00042-6**

Lohmar, S., Parada, M., Gutiérrez, F., Robin, C., & Gerbe, M. C. (2012). Mineralogical and numerical approaches to establish the pre-eruptive conditions of the mafic Licán Ignimbrite, Villarrica Volcano (Chilean Southern Andes). Journal of Volcanology and Geothermal Research, 235, 55-69. doi: **https://doi.org/10.1016/j.jvolgeores.2012.05.006**

López-Ramos, E. (1979). Geología de México. UNAM, México.

Lucci, F., Carrasco-Núñez, G., Rossetti, F., Theye, T., White, J. C., Urbani, S., ... & Giordano, G. (2020). Anatomy of the magmatic plumbing system of Los Humeros Caldera (Mexico): implications for geothermal systems. Solid Earth, 11(1), 125-159. doi: **https://doi.org/10.5194/se-11-125-2020**

Macías, J. L. (2007). Geology and eruptive history of some active volcanoes of México. En C. C. Susana A. Alaniz-Álvarez, Ángel F. Nieto-Samaniego (Eds.) Geology of México: Celebrating the Centenary of the Geological Society of México. Geological Society of America. doi: **https://doi.org/10.1130/2007.2422(06)**

Macías, J. L., Sosa-Ceballos, G., Arce, J. L., Gardner, J. E., Saucedo, R., & Valdez-Moreno, G. (2017). Storage conditions and magma processes triggering the 1818 CE Plinian eruption of Volcán de Colima. Journal of Volcanology and Geothermal Research, 340, 117-129. doi: **https://doi.org/10.1016/j.jvolgeores.2017.02.025**

Marxer, F., Ulmer, P., & Müntener, O. (2022). Polybaric fractional crystallisation of arc magmas: an experimental study simulating trans-crustal magmatic systems. Contributions to Mineralogy and Petrology, 177(1), 3. doi: **https://doi.org/10.1007/s00410-021-01856-8**

Moore, G., & Carmichael, I. S. E. (1998). The hydrous phase equilibria (to 3 kbar) of an andesite and basaltic andesite from western Mexico: constraints on water content and conditions of phenocryst growth. Contributions to Mineralogy and Petrology, 130(3), 304-319. doi: **https://doi.org/10.1007/s004100050367**

Mooser, F. (1972). The mexican volcanic belt structure and tectonicas. Geofísica Internacional, 12(2), 55-70. doi: **https://doi.org/10.22201/igeof.00167169p.1972.12.2.1024**

Morgavi, D., Laumonier, M., Petrelli, M., & Dingwell, D. B. (2022). Decrypting magma mixing in igneous systems. Reviews in Mineralogy and Geochemistry, 87(1), 607-638. doi: **https://doi.org/10.2138/rmg.2022.87.13**

Muir, D. D., Blundy, J. D., Rust, A. C., & Hickey, J. (2014). Experimental constraints on dacite pre-eruptive magma storage conditions beneath Uturuncu volcano. Journal of Petrology, 55(4), 749-767. doi: **https://doi.org/10.1093/petrology/egu005**

Nelson, S. T., & Montana, A. (1992). Sieve-textured plagioclase in volcanic rocks produced by rapid decompression. American Mineralogist, 77(11-12), 1242-1249.

Newman, S., & Lowenstern, J. B. (2002). VolatileCalc: a silicate melt–H2O–CO2 solution model written in Visual Basic for excel. Computers & Geosciences, 28(5), 597-604. doi: **https://doi.org/10.1016/S0098-3004(01)00081-4**

Nielsen, R. L. (1988). A model for the simulation of combined major and trace element liquid lines of descent. Geochimica et Cosmochimica Acta, 52(1), 27-38. doi: **https://doi.org/10.1016/0016-7037(88)90053-1**

Oba, T. (1990). Experimental study on the tremolite-pargasite join at variable temperatures under 10 kbar. Proceedings of the Indian Academy of Sciences-Earth and Planetary Sciences, 99, 81-90. **https://doi.org/10.1007/BF02871897**

Papoutsa, A., & Pe-Piper, G. (2014). Geochemical variation of amphiboles in A-type granites as an indicator of complex magmatic systems: Wentworth pluton, Nova Scotia, Canada. Chemical Geology, 384, 120-134. doi: **https://doi.org/10.1016/j.chemgeo.2014.07.001**

Pelullo, C., Iovine, R. S., Arienzo, I., Di Renzo, V., Pappalardo, L., Petrosino, P., & D'Antonio, M. (2022). Mineral-melt equilibria and geothermobarometry of Campi Flegrei magmas: Inferences for magma storage conditions. Minerals, 12(3), 308. doi: **https://doi.org/10.3390/min12030308**

Philpotts, A. R., & Ague, J. J. (2009). Principles of Igneous and Metamorphic Petrology (2a ed.). Cambridge University Press.

Price, R. C., Gamble, J. A., Smith, I. E., Maas, R., Waight, T., Stewart, R. B., & Woodhead, J. (2012). The anatomy of an andesite volcano: a time–stratigraphic study of andesite petrogenesis and crustal evolution at Ruapehu Volcano, New Zealand. Journal of Petrology, 53(10), 2139-2189. doi: **https://doi.org/10.1093/petrology/egs050**

Price, R. C., Gamble, J. A., Smith, I. E., Stewart, R. B., Eggins, S., & Wright, I. C. (2005). An integrated model for the temporal evolution of andesites and rhyolites and crustal development in New Zealand's North Island. Journal of Volcanology and Geothermal Research, 140(1-3), 1-24. doi: **https://doi.org/10.1016/j.jvolgeores.2004.07.013**

Reiners, P. W., Nelson, B. K., & Ghiorso, M. S. (1995). Assimilation of felsic crust by basaltic magma: thermal limits and extents of crustal contamination of mantle-derived magmas. Geology, 23(6), 563-566. doi: **https://doi.org/10.1130/0091-7613(1995)023<0563:AOFCBB>2.3.CO;2**

Reubi, O., & Blundy, J. (2008). Assimilation of plutonic roots, formation of high-K 'exotic' melt inclusions and genesis of andesitic magmas at Volcán de Colima, Mexico. Journal of Petrology, 49(12), 2221-2243. doi: **https://doi.org/10.1093/petrology/egn066**

Reubi, O., & Blundy, J. (2009). A dearth of intermediate melts at subduction zone volcanoes and the petrogenesis of arc andesites. Nature, 461(7268), 1269-1273. doi: **https://doi.org/10.1038/nature08510**

Ridolfi, F., & Renzulli, A. (2012). Calcic amphiboles in calc-alkaline and alkaline magmas: thermobarometric and chemometric empirical equations valid up to 1,130° C and 2.2 GPa. Contributions to Mineralogy and Petrology, 163, 877-895. doi: **https://doi.org/10.1007/s00410-011-0704-6**

Ridolfi, F., Renzulli, A., & Puerini, M. (2010). Stability and chemical equilibrium of amphibole in calc-alkaline magmas: an overview, new thermobarometric formulations and application to subduction-related volcanoes. Contributions to mineralogy and petrology, 160, 45-66. doi: **https://doi.org/10.1007/s00410-009-0465-7**

Rollison, H. R. (1993). Using geochemical data: Evaluation, presentation, interpretation. Longman Scientific & Technical

Rudnick R. L. & Gao S. (2003) Composition of the continental crust. In The Crust, vol. 3 (ed. R. L. Rudnick). Elsevier Science. doi: **https://doi.org/10.1016/B0-08-043751-6/03016-4**

Rutherford, M. J. (1993). Experimental petrology applied to volcanic processes. Eos, Transactions American Geophysical Union, 74(5), 49-55. doi: **https://doi.org/10.1029/93EO00142**

Rutherford, M. J., & Devine, J. D. (2003). Magmatic conditions and magma ascent as indicated by hornblende phase equilibria and reactions in the 1995–2002 Soufriere Hills magma. Journal of petrology, 44(8), 1433-1453. doi: **https://doi.org/10.1093/petrology/44.8.1433**

Schaaf, P., Stimac, J. I. M., Siebe, C., & Macías, J. L. (2005). Geochemical evidence for mantle origin and crustal processes in volcanic rocks from Popocatépetl and surrounding monogenetic volcanoes, central Mexico. Journal of Petrology, 46(6), 1243-1282. doi: **https://doi.org/10.1093/petrology/egi015**

Schneider, C. A., Rasband, W. S., & Eliceiri, K. W. (2012). NIH Image to ImageJ: 25 years of image analysis. Nature methods, 9(7), 671-675. doi: **https://doi.org/10.1038/nmeth.2089**

Seele, E., & Mooser, F. (1972). La Malinche y la tectónica del valle de Puebla. Memorias de la II Convención Nacional de la Sociedad Geológica Mexicana, 234-235.

Sigurdsson, H., Carey, S. N., & Espindola, J. M. (1984). The 1982 eruptions of El Chichón volcano, Mexico: stratigraphy of pyroclastic deposits. Journal of Volcanology and Geothermal Research, 23(1-2), 11-37. doi: **https://doi.org/10.1016/0377-0273(84)90055-6**

Singer, B. S., Jicha, B. R., Harper, M. A., Naranjo, J. A., Lara, L. E., & Moreno-Roa, H. (2008). Eruptive history, geochronology, and magmatic evolution of the Puyehue-Cordón Caulle volcanic complex, Chile. Geological Society of America Bulletin, 120(5-6), 599-618. doi: **https://doi.org/10.1130/B26276.1**

Sisson, V. B., Hollister, L. S., & Onstott, T. C. (1989). Petrologic and age constraints on the origin of a low-pressure/high-temperature metamorphic complex, southern Alaska. Journal of Geophysical Research: Solid Earth, 94(B4), 4392-4410. doi: **https://doi.org/10.1029/JB094iB04p04392**

Sosa-Ceballos, G., Gardner, J. E., & Lassiter, J. C. (2014). Intermittent mixing processes occurring before Plinian eruptions of Popocatepetl volcano, Mexico: insights from textural–compositional variations in plagioclase and Sr–Nd–Pb isotopes. Contributions to Mineralogy and Petrology, 167, 1-19. doi: **https://doi.org/10.1007/s00410-014-0966-x**

Sosa-Ceballos, G., Gardner, J. E., Siebe, C., & Macías, J. L. (2012). A caldera-forming eruption~ 14,100 14C yr BP at Popocatépetl volcano, México: Insights from eruption dynamics and magma mixing. Journal of Volcanology and Geothermal Research, 213, 27-40. doi: **https://doi.org/10.1016/j.jvolgeores.2011.11.001**

Speer, J. A. (1987). Evolution of magmatic AFM mineral assemblages in granitoid rocks; the hornblende+ melt= biotite reaction in the Liberty Hill Pluton, South Carolina. American Mineralogist, 72(9-10), 863-878.

Spilliaert, N., Allard, P., Métrich, N., & Sobolev, A. V. (2006). Melt inclusion record of the conditions of ascent, degassing, and extrusion of volatile-rich alkali basalt during the powerful 2002 flank eruption of Mount Etna (Italy). Journal of Geophysical Research: Solid Earth, 111(B4). doi: **https://doi.org/10.1029/2005JB003934**

Stephenson, D. (1993). Amphiboles from Dalradian metasedimentary rocks of NE Scotland: Environmental inferences and distinction from amphiboles of meta-igneous amphibolites. Mineralogy and Petrology, 49(1-2), 45-62. doi: **https://doi.org/10.1007/BF01162925**

Streck, M. J., Leeman, W. P., & Chesley, J. (2007). High-magnesian andesite from Mount Shasta: a product of magma mixing and contamination, not a primitive mantle melt. Geology, 35(4), 351-354. doi: **https://doi.org/10.1130/G23286A.1**

Taylor Jr, H. P. (1980). The effects of assimilation of country rocks by magmas on 18O/16O and 87Sr/86Sr systematics in igneous rocks. Earth and Planetary Science Letters, 47(2), 243-254. doi: **https://doi.org/10.1016/0012-821X(80)90040-0**

Tepley Iii, F. J., Davidson, J. P., & Clynne, M. A. (1999). Magmatic interactions as recorded in plagioclase phenocrystals of Chaos Crags, Lassen Volcanic Center, California. Journal of Petrology, 40(5), 787-806. doi: **https://doi.org/10.1093/petroj/40.5.787**

Tomiya, A., Takahashi, E., Furukawa, N., & Suzuki, T. (2010). Depth and evolution of a silicic magma chamber: melting experiments on a low-K rhyolite from Usu Volcano, Japan. Journal of Petrology, 51(6), 1333-1354. doi: **https://doi.org/10.1093/petrology/egq021**

Underwood, S. J., Feeley, T. C., & Clynne, M. A. (2012). Hydrogen isotope investigation of amphibole and biotite phenocrystals in silicic magmas erupted at Lassen Volcanic Center, California. Journal of volcanology and geothermal research, 227, 32-49. doi: **https://doi.org/10.1016/j.jvolgeores.2012.02.019**

Viccaro, M., Giacomoni, P. P., Ferlito, C., & Cristofolini, R. (2010). Dynamics of magma supply at Mt. Etna volcano (Southern Italy) as revealed by textural and compositional features of plagioclase phenocrysts. Lithos, 116(1-2), 77-91. doi: **https://doi.org/10.1016/j.lithos.2009.12.012**

Werner, G. (1976). La Desforestacion en el volcán" La Malinche" y sus consecuencias en el desarrollo de los suelos asi como en sus propiedades ecológicas.

Winter, J. D. (2014). Principles of Igneous and Metamorphic Petrology (2a ed.). Pearson.

Yazdi, A., Ashja Ardalan, A., Emami, M. H., Dabiri, R., & Foudazi, M. (2019). Magmatic interactions as recorded in plagioclase phenocrystals of quaternary volcanics in SE Bam (SE Iran). Iranian Journal of Earth Sciences, 11(3), 215-225.

Zajacz, Z., Halter, W. E., Pettke, T., & Guillong, M. (2008). Determination of fluid/melt partition coefficients by LA-ICPMS analysis of co-existing fluid and silicate melt inclusions: Controls on element partitioning. Geochimica et Cosmochimica Acta, 72(8), 2169-2197. doi: **https://doi.org/10.1016/j.gca.2008.01.034**

Zajacz, Z., Hanley, J. J., Heinrich, C. A., Halter, W. E., & Guillong, M. (2009). Diffusive reequilibration of quartz-hosted silicate melt and fluid inclusions: Are all metal concentrations unmodified?. Geochimica et Cosmochimica Acta, 73(10), 3013-3027. doi: **https://doi.org/10.1016/j.gca.2009.02.023**

Zellmer, G. F., Rubin, K. H., & Gronvold, K. (2008). On the recent bimodal magmatic processes and their timescales in the Torfajökull central volcano, Iceland. Journal of Volcanology and Geothermal Research, 170(3-4), 152-169.